Advances in Bioresearch
Adv. Biores., Vol 17 (4) April 2026: 90-115

Print ISSN 0976-4585; Online ISSN 2277-1573
Journal's URL:http://www.soeagra.com/abr.html
CODEN: ABRDC3
DOI: 10.15515/abr.0976-4585.17.4.90115

Advances in Bioresearch

ORIGINAL ARTICLE

Integrated Phytochemical and Computational Investigation of *Cissus verticillata* as a Natural DPP-IV Inhibitor

Kedar Kailas Ganjare[1]*, Sharad D. Tayade[2], Arfin S. Tamboli[1], Inzamamul Haq Ameer Shaikh[1], Vijay S. Borkar[3], Jyoti Bhushan Khedekar[4]**

[1] Research Scholar, Department of Industrial Pharmacy, Shri Sant Gajanan Maharaj College of Pharmacy, Buldana-443001, Maharashtra, India

[*2] Department of Industrial Pharmacy, Shri Sant Gajanan Maharaj College of Pharmacy, Buldana-443001, Maharashtra, India

[3] Department of Pharmaceutical Chemistry, Shri Sant Gajanan Maharaj College of Pharmacy, Buldana-443001, Maharashtra, India

[4] Department of Pharmaceutics, Shri Sant Gajanan Maharaj College of Pharmacy, Buldana-443001, Maharashtra, India

***Correspondence author email:** kedarganjare@gmail.com; sharad_tayade1@rediffmail.com

ABSTRACT

The present study aimed to evaluate the phytochemical composition, physicochemical properties, microbial safety, and in silico antidiabetic potential of Cissus verticillata. The plant extract was obtained using hydroalcoholic Soxhlet extraction with a yield of 9.8%. Physicochemical analysis showed slightly acidic pH (5.8 for 1% and 5.2 for 10% solution), low foreign content (0.4%), and loss on drying (6.9%). Ash values were within acceptable limits, including total ash (11.4%), acid-insoluble ash (2.5%), water-soluble ash (5.24%), and sulphated ash (9.52%). Extractive values indicated higher water-soluble extractives (27.75%) compared to alcohol-soluble extractives (18.91%), with absence of heavy metals and pesticide residues. Qualitative phytochemical screening revealed the presence of carbohydrates (++), flavonoids (+++), phenolic compounds (+++), tannins (++), and saponins (++), while fats and anthraquinone glycosides were absent. Microbial analysis confirmed the absence of Escherichia coli, Salmonella spp., Shigella spp., Pseudomonas aeruginosa, and Staphylococcus aureus. GC–MS analysis identified major compounds such as 1,2,3-benzenetriol (~13.76%) and γ-sitosterol (~6.34%), along with phenolics, fatty acids, terpenoids, and phytosterols. Molecular docking studies against DPP-IV (PDB ID: 1X70) revealed strong binding affinity of stigmasterol (−9.6 kcal/mol), campesterol (−9.4 kcal/mol), and γ-sitosterol (−9.2 kcal/mol). ADMET analysis indicated favorable pharmacokinetic properties for phenolic compounds, while sterols showed high lipophilicity. Overall, Cissus verticillata demonstrates significant potential as a natural source of antidiabetic agents.

KEYWORDS: *Cissus verticillata*; Phytochemical screening; GC–MS analysis; Molecular docking; DPP-IV inhibition; ADMET analysis

Received 24.01.2026 Revised 01.02.2026 Accepted 11.02.2026

How to cite this article:
Kedar Kailas G, Sharad D. T, Arfin S. T, Inzamamul Haq A S, Vijay S. B, Jyoti Bhushan K. Integrated Phytochemical and Computational Investigation of *Cissus verticillata* as a Natural DPP-IV Inhibitor. Adv. Biores. Vol 17 [4] April 2026. 90-115

INTRODUCTION

Diabetes mellitus is a chronic metabolic disorder characterized by persistent hyperglycemia resulting from impaired insulin secretion, insulin resistance, or both [1]. It is associated with severe complications such as neuropathy, nephropathy, retinopathy, and cardiovascular diseases, posing a significant global health burden [2–4]. Among various therapeutic targets, dipeptidyl peptidase-IV (DPP-IV) has gained considerable attention due to its role in the degradation of incretin hormones such as glucagon-like peptide-1 (GLP-1) [5–7]. Inhibition of DPP-IV prolongs incretin activity, enhances insulin secretion, and improves glycemic control, making it an effective strategy in the management of type 2 diabetes mellitus [8,9]. Currently available synthetic DPP-IV inhibitors, although effective, are often associated with limitations such as adverse effects, high cost, and long-term safety concerns [10,11]. This has led to

growing interest in identifying natural, plant-derived compounds as safer and cost-effective alternatives [12]. Medicinal plants are rich sources of bioactive phytoconstituents, including phenolics, flavonoids, alkaloids, terpenoids, and glycosides, which have demonstrated significant antidiabetic potential through multiple mechanisms, including enzyme inhibition and antioxidant activity [12].

Cissus verticillata, a medicinal plant belonging to the Vitaceae family, has been traditionally used in various herbal systems for its therapeutic properties. It is known to possess a wide range of pharmacological activities, including antidiabetic, anti-inflammatory, antioxidant, and antimicrobial effects. Previous studies have reported the presence of diverse phytochemicals such as flavonoids, tannins, phenolic compounds, terpenoids, and phytosterols in *Cissus verticillata*, which are believed to contribute to its biological activities [13,14]. However, systematic evaluation of its DPP-IV inhibitory potential using integrated experimental and computational approaches remains limited. Phytochemical screening and physicochemical analysis are essential steps in establishing the identity, purity, and quality of plant extracts, while advanced analytical techniques such as gas chromatography–mass spectrometry (GC–MS) enable the identification of individual bioactive compounds. Furthermore, computational tools such as molecular docking and ADMET (Absorption, Distribution, Metabolism, Excretion, and Toxicity) analysis provide valuable insights into the interaction of phytoconstituents with target proteins and their pharmacokinetic behavior, thereby accelerating drug discovery processes [15–17].

In this context, the present study aims to perform an integrated investigation of *Cissus verticillata* by combining phytochemical characterization, physicochemical evaluation, microbial safety assessment, GC–MS analysis, and in silico computational studies. The study specifically focuses on evaluating the binding affinity of identified phytoconstituents toward the DPP-IV enzyme and assessing their drug-likeness and pharmacokinetic properties. This integrated approach is expected to provide a comprehensive understanding of the therapeutic potential of *Cissus verticillata* and support its development as a natural source of DPP-IV inhibitors for the management of diabetes mellitus.

MATERIAL AND METHODS

Collection of Plant Material and Authentication

Cissus verticillata herb was collected in December 2024 from a local area of Buldhana, Maharashtra, India. The collected plant material was processed for herbarium preparation and subsequently authenticated by the Department of Botany, Government Degree College, Kukatpally, Medchal District, Telangana (affiliated to Osmania University). The authentication was performed by P. Suresh Babu, Assistant Professor of Botany. A voucher specimen (No. 0937) was assigned and preserved for future reference. The authentication certificate was issued on 13.03.2026. After authentication, the plant material was used for further extraction studies. The images of the plant are presented in Figure 1.

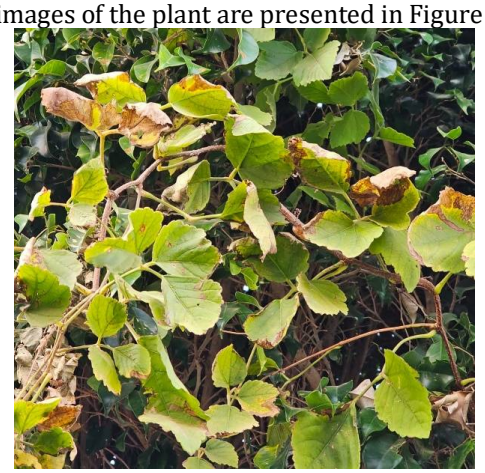

Figure 1: The *Cissus verticillata* plant

Soxhlet Extraction using Hydroalcoholic Solvent

For extraction, *Cissus verticillata's* leaves and bark were collected and washed them using distilled water to remove any dust or foreign particle, and then air-dried in the shade for a week at room temperature. It is essential to dry it in room temperature to avoid the loss of volatile phytoconstituents. About 500 grams of dried plant material was grinded into a course powder for further extraction process. The resulting powder was subjected for Soxhlet extraction using Soxhlet apparatus by hydroalcoholic solvent (Ethanol:water; 70:30). The extraction process was continued until complete isolation of secondary metabolites present in plant material. The dark green color of the solvent in RBF and fainted color of plant material in Soxhlet extractor denoted the successive isolation of constituents [18,19]. At least 24

hours were devoted for the extraction and during this meantime several siphon cycles were completed. The contents of the RFB then poured into different petri plates and the solvent was allowed to evaporate naturally for few hours. The concentrated extract was then subjected for different qualitative analysis tests. The working photographs of Soxhlet extraction are depicted in Figure 2.

Figure 2: The Soxhlet extraction of *Cissus verticillata*

Physicochemical Analysis

Color of unprocessed extract was observed under natural light. Odor assessed by deep breaths over small sample; taste by swishing on tongue. pH of 1% and 10% solutions (0.1 g extract in 10 mL distilled water, filtered as needed) measured with digital pH meter. Foreign content in 0.1 g powder separated, weighed, percentage calculated. Loss on drying: 0.3 g powder dried at 105°C to constant weight. Ash values (air-dried drug basis): total (3 g incinerated ≤450°C constant weight); acid-insoluble (total ash boiled 25 mL dilute HCl 5 min, filtered, incinerated); sulphated (1 g charred, H_2SO_4 treated, 800±25°C to <0.5 mg difference); water-soluble (total ash boiled 25 mL water 5 min, insoluble filtered, incinerated).

Extractives (5 g powder, shaker maceration 6 h): alcohol-soluble (100 mL 90% alcohol, filtrate evaporated); water-soluble (100 mL chloroform water + overnight, filtrate evaporated); percentages from residues. Heavy metals (As, Cd, Pb, Hg, Zn, Cu, Cr, Mn) in 5 g powder digested 3 M HNO_3, diluted 50 mL, AAS (air-acetylene, triplicate standards). Pesticides: rotary evaporated, cleaned, 5 mL hexane, GC-ECD (0.1–0.5 ppb) [18,19].

Qualitative Phytochemical Screening

The extract was subjected to qualitative phytochemical screening using standard chemical tests to identify major classes of phytoconstituents. Carbohydrates were detected by Molisch's test (violet ring), while reducing sugars and monosaccharides were confirmed by Fehling's, Benedict's, and Barfoed's tests through red precipitate formation. Proteins and amino acids were identified using Biuret, Millon's, Xanthoprotein, and Ninhydrin tests based on characteristic color changes. Fats and oils were confirmed by saponification test (soap formation). Steroids were detected using Salkowski and Liebermann–Burchard reactions showing color changes. Cardiac glycosides and anthraquinone glycosides were identified by Keller–Killiani and Borntrager's tests, respectively. Saponins showed persistent foam, while cyanogenic glycosides were detected using sodium picrate paper. Flavonoids were confirmed by Shinoda and lead acetate tests (yellow precipitate). Alkaloids were identified using Dragendorff's, Mayer's, Wagner's, and Hager's tests through precipitate formation. Tannins and phenolics were detected using ferric chloride and related tests by color change or precipitate formation. These tests confirmed the presence of key phytochemical constituents in the extract [20].

Microbial Content Determination

Microbial load of the samples was determined using the standard plate count method. For solid samples, 1 g of the powder was dispersed in 9 mL of sterile distilled water, while for liquid samples, 1 mL was diluted in 9 mL of sterile distilled water. Serial dilutions were prepared, and microbial viability was assessed using the pour plate method. The inoculated plates were incubated at 37°C for 24 h, and colonies were counted using a colony counter. The microbial content was expressed as the mean of duplicate determinations. Selective media such as Nutrient agar, Cetrimide agar, Salt agar, and MacConkey agar were used for bacterial enumeration. For fungal detection, Sabouraud dextrose agar plates were prepared, and 1 mL of sample was spread on the surface and incubated at 27°C for 72 h. Detection of specific microorganisms was carried out using enrichment and selective culture techniques. For Escherichia coli, the sample was enriched in nutrient broth at 37°C for 24 h, followed by inoculation into MacConkey broth and incubation for 48 h, where acid and gas production indicated its presence. For Salmonella spp., enrichment was done in nutrient broth, followed by subculture in Selenite and Tetrathionate broths, and plating on Deoxycholate citrate agar with incubation at 36–38°C. For Shigella spp., enrichment was performed in nutrient broth (pH 8.0) at 37°C for 18 h, followed by streaking on Salmonella–Shigella agar and confirmation using biochemical tests such as TSI agar. Detection of Pseudomonas aeruginosa involved enrichment in soybean-casein digest medium, followed by plating on Cetrimide agar and confirmation by oxidase test. For Staphylococcus aureus, the sample was enriched in peptone water, streaked on Mannitol Salt Agar, incubated at 37°C, and confirmed using catalase and coagulase tests. These procedures were used for comprehensive evaluation of microbial contamination and identification of specific microorganisms in the samples [21,22].

GC-MS Analysis

GC–MS analysis of *Cissus verticillata* extract was performed to identify volatile and semi-volatile phytoconstituents. The filtered extract was injected (1.0 µL) into a GC–MS system equipped with an electron ionization (EI) source using an auto-sampler in split mode. Separation was achieved on a capillary column with helium as the carrier gas at a constant flow rate. The oven temperature was programmed to increase gradually to ensure effective separation of compounds based on volatility. The injector and ion source temperatures were optimized for proper vaporization and ionization. The mass spectrometer operated in EI mode (70 eV) with a suitable scan range to detect compounds across different mass-to-charge ratios. Compound identification was carried out by comparing obtained mass spectra with standard NIST library data. Data acquisition and processing were performed using dedicated instrument software, ensuring reproducibility and reliability of the analytical procedure [19].

Molecular Docking

Molecular docking analysis was performed to evaluate the binding affinity of phytoconstituents from *Cissus verticillata* against DPP-IV. The three-dimensional structure of the target protein DPP-IV (PDB ID: 1X70) was retrieved from the Protein Data Bank (PDB). The protein structure was prepared by removing water molecules, ligands, and heteroatoms, followed by the addition of hydrogen atoms and energy minimization using Discovery Studio [23–25]. The chemical structures of selected compounds were obtained from PubChem and drawn or optimized using ChemDraw. The ligands were converted into

appropriate file formats and energy minimized prior to docking. Docking simulations were carried out using PyRx integrated with AutoDock Vina. The grid box was defined around the active site of the protein with center coordinates set at X = 41.184143, Y = 51.045036, and Z = 35.628679 to ensure proper ligand binding orientation. The docking process generated multiple binding conformations, and the best poses were selected based on binding affinity scores and interaction profiles. Visualization and analysis of protein–ligand interactions were performed using Discovery Studio to evaluate hydrogen bonding, hydrophobic interactions, and binding stability. Active cavity of DPP-IV with Native Ligand are seen in Figure 3.

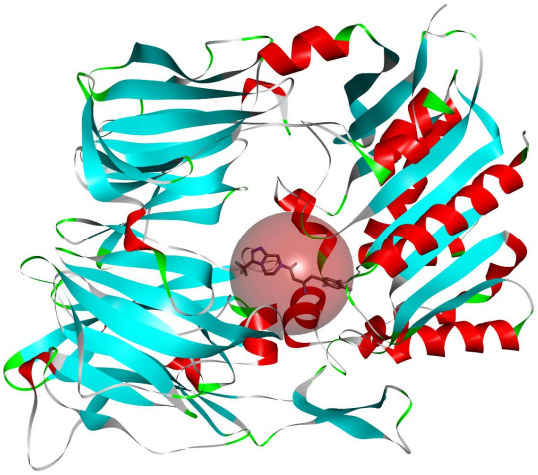

Figure 3: Three-dimensional representation of the active binding cavity of DPP-IV (PDB ID: 1X70) showing the native ligand within the catalytic site

ADMET Analysis

The ADMET (Absorption, Distribution, Metabolism, Excretion, and Toxicity) analysis of selected phytoconstituents from *Cissus verticillata* was performed to evaluate their drug-likeness and pharmacokinetic properties. The chemical structures of the compounds were retrieved from PubChem and, where necessary, drawn and optimized using ChemDraw. The prepared ligand structures were converted into appropriate formats (SMILES) and subjected to in silico ADMET prediction. Drug-likeness and physicochemical properties, including Lipinski's rule of five, bioavailability, and permeability, were assessed using SwissADME. Further pharmacokinetic parameters such as absorption, distribution, metabolism, excretion, and toxicity profiles were evaluated using ADMETlab 3.0. All predictions were carried out under default parameters of the respective tools. The results obtained were used to assess the suitability of the compounds as potential DPP-IV inhibitors based on their pharmacokinetic behavior and safety profile [26,27].

RESULTS AND DISCUSSION

Organoleptic and Physicochemical Analysis of Extracts

The hydroalcoholic extract of *Cissus verticillata* exhibited characteristic organoleptic properties, including a green to dark brown colour, herbal and mildly bitter odour, and slightly astringent to bitter taste. The colour variation may be attributed to the presence of chlorophyll along with oxidized phenolic compounds. The observed odour and taste indicate the presence of bioactive constituents such as tannins and flavonoids. The extract showed a semi-solid, sticky texture, suggesting the presence of resinous substances and polysaccharides. The percentage yield of 9.8% reflects efficient extraction of phytoconstituents using a hydroalcoholic solvent system. Physicochemical evaluation revealed that the extract possesses a slightly acidic pH (5.8 for 1% solution and 5.2 for 10% solution), which is favorable for the stability of phenolic compounds and may also help in limiting microbial growth. The foreign content was found to be low (0.4%), indicating minimal contamination and proper handling of the plant material. The loss on drying (6.9%) suggests low moisture content, which is beneficial for enhancing shelf life and preventing microbial degradation. The ash values provide insight into the inorganic composition of the extract. The total ash value (11.4%) indicates overall mineral content, while the acid insoluble ash (2.5%) reflects minimal siliceous impurities such as sand and soil. The water-soluble ash (5.24%) denotes the presence of soluble inorganic salts, and the sulphated ash value (9.52%) confirms the presence of stable mineral residues. These parameters collectively indicate acceptable purity and quality of the extract. The extractive values demonstrated a higher water-soluble extractive value (27.75%) compared to the alcohol-soluble extractive (18.91%), suggesting the predominance of polar constituents such as

glycosides, tannins, sugars, and phenolic compounds. This indicates that aqueous components play a major role in the phytochemical composition of the extract. Furthermore, the absence of heavy metals and pesticide residues confirms that the extract is free from toxic contaminants and is safe for pharmaceutical applications. Overall, the observed organoleptic and physicochemical parameters comply with standard pharmacognostic limits, supporting the identity, purity, and quality of *Cissus verticillata* extract for further therapeutic and formulation studies. Physicochemical analysis of *Cissus verticillata* are shown in Figure 4.

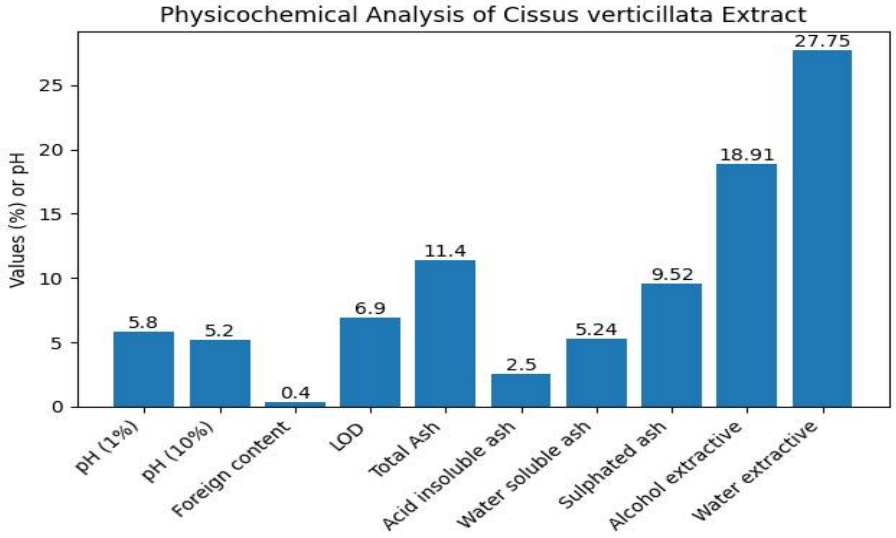

Figure 4: Physicochemical analysis of *Cissus verticillata*

Qualitative Phytochemical Screening

The qualitative phytochemical screening of *Cissus verticillata* extract revealed the presence of diverse bioactive constituents (5). The extract showed moderate presence of carbohydrates and reducing sugars (++), along with trace levels of monosaccharides (+), indicating the presence of soluble sugars and glycosidic components. Proteins and amino acids were detected in low amounts (+), suggesting limited nutritional contribution. The extract tested negative for fats and oils (-), indicating the negligible presence of non-polar lipid components. Steroids and cardiac glycosides were present in trace amounts (+), which may contribute to certain pharmacological activities. Saponin glycosides were moderately present (++), suggesting potential roles in membrane permeability and antimicrobial action. Alkaloids were detected in low amounts (+), whereas anthraquinone glycosides were absent (-), indicating that laxative-type constituents are not significant in this extract. Notably, phenolic compounds and flavonoids were found in abundant amounts (+++), identifying them as the phytoconstituents likely responsible for antioxidant activity. Tannins were moderately present (++), contributing to the astringent characteristics of the extract. Overall, the phytochemical profile indicates the predominance of polar secondary metabolites, particularly phenolics and flavonoids, which supports the potential therapeutic efficacy of *Cissus verticillata* extract.

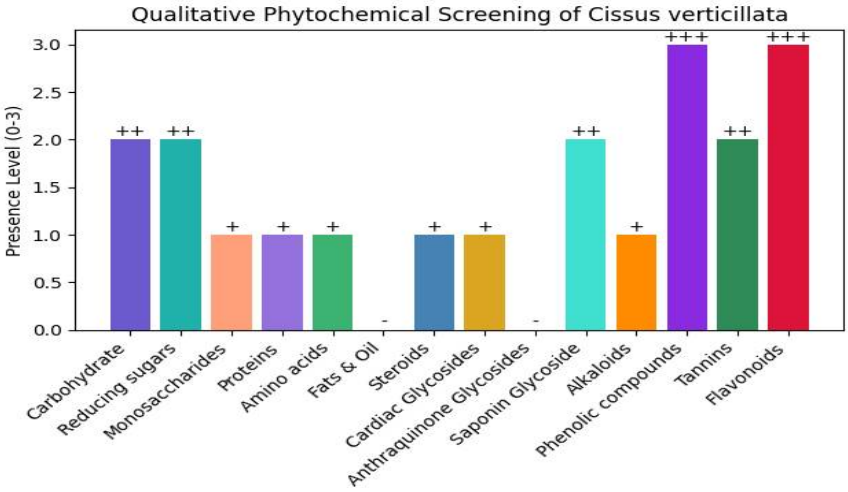

Figure 5: Qualitative phytochemical screening of *Cissus verticillata*

Microbial Content Determination

The microbial analysis of *Cissus verticillata* extract demonstrated the absence of all tested pathogenic microorganisms. Specifically, Escherichia coli, Salmonella spp., Shigella spp., Pseudomonas aeruginosa, and Staphylococcus aureus were not detected in the sample. The absence of these microorganisms indicates that the extract meets acceptable microbiological quality standards and reflects proper handling, processing, and hygienic conditions during extraction. The lack of E. coli and Salmonella spp. confirms the absence of fecal contamination, while the non-detection of Shigella spp. further supports the microbiological safety of the sample. Additionally, the absence of Pseudomonas aeruginosa and Staphylococcus aureus suggests minimal risk of opportunistic infections and contamination from environmental or handling sources. Overall, these findings confirm that the extract is microbiologically safe and suitable for pharmaceutical or nutraceutical applications, supporting its quality, safety, and compliance with standard microbial limits.

GC-MS Analysis

The GC–MS analysis of the hydroalcoholic extract of *Cissus verticillata* revealed a diverse range of phytoconstituents distributed across the chromatographic run from approximately 1.5 to 58.7 min. The chromatogram exhibited several well-resolved peaks corresponding to compounds of varying polarity and molecular weight. In the early retention time region, volatile compounds such as methylene chloride (RT ~1.77 min; ~30.47% area) and pentanoic acid, 3-methyl-4-oxo (RT ~2.18 min; ~17.50% area) were predominant. These compounds indicate the presence of low molecular weight organic constituents. The region of the chromatogram was dominated by phenolic compounds, including 2-methoxy-4-vinylphenol (RT ~19.40 min; ~0.12% area) and 1,2,3-benzenetriol (RT ~21.64 min; ~13.76% area), with the latter representing a major peak. The presence of substituted phenols such as 3,5-di-tert-butylphenol (RT ~25.78 min; ~0.41% area) further confirms the phenolic richness of the extract. In the mid to late retention region, fatty acids and their derivatives were identified, including tetradecanoic acid (RT ~31.98 min; ~0.16% area), n-hexadecanoic acid (RT ~34.71 min; ~2.66% area), and 9,12-octadecadienoic acid methyl ester (RT ~36.50 min; ~0.55% area). Terpenoid compounds such as neophytadiene (RT ~32.99 min; ~0.53% area) and phytol (RT ~36.80 min; ~0.77% area) were also detected. At higher retention times, phytosterols were prominently observed, including campesterol (RT ~53.38 min; ~1.35% area), stigmasterol (RT ~53.72 min; ~0.97% area), and γ-sitosterol (RT ~54.52 min; ~6.34% area), indicating the abundance of sterol components in the extract. Overall, the GC–MS results confirm that *Cissus verticillata* extract is rich in phenolics, fatty acids, terpenoids, and phytosterols, with major contributions from 1,2,3-benzenetriol and γ-sitosterol, highlighting its significant phytochemical diversity and potential biological activity. The graph of GC-MS analysis is shown in Figure 6. and Compound Identified in GC-MS analysis for *Cissus verticillata* extract are shown in Table 1.

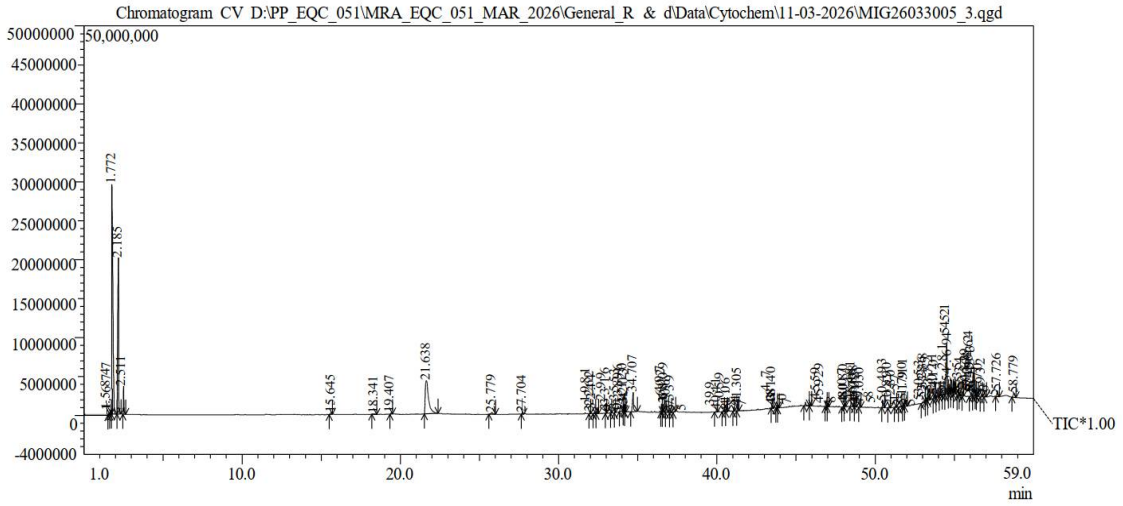

Figure 6: Graph of GC-MS Analysis

Table 1: GC–MS identified phytoconstituents of *Cissus verticillata* extract with retention time, molecular classification, and identification rationale

Sr. No.	RT (min)	Compound Name	Molecular Type	Rationale
1	2.185	Pentanoic acid, 3-methyl-4-oxo	Organic acid	Early RT with keto-acid fragmentation
2	19.407	2-Methoxy-4-vinylphenol	Phenolic compound	Typical phenolic fragmentation
3	21.638	1,2,3-Benzenetriol	Phenolic compound	Major peak (~13.76%), strong phenolic signal
4	25.779	Phenol, 3,5-bis(1,1-dimethylethyl)	Phenolic antioxidant	Bulky substituted phenol
5	31.981	Tetradecanoic acid	Fatty acid	Saturated fatty acid fragmentation pattern
6	32.990	Neophytadiene	Diterpene	Characteristic hydrocarbon terpenoid
7	33.553	3,7,11,15-Tetramethyl-2-hexadecen-1-ol	Terpenoid alcohol	Isoprenoid chain fragmentation
8	33.896	Benzoic acid, 3,4,5-trihydroxy-, methyl ester	Phenolic ester	Polyhydroxy aromatic ester
9	34.707	n-Hexadecanoic acid	Fatty acid	Major fatty acid (~2.66% area)
10	36.497	9,12-Octadecadienoic acid, methyl ester	Fatty acid ester	Unsaturated fatty acid signature
11	53.383	Campesterol	Phytosterol	Plant sterol fingerprint
12	53.722	Stigmasterol	Phytosterol	Unsaturated sterol structure
13	54.521	γ-Sitosterol	Phytosterol	Major sterol (~6.34% area)

Molecular Docking

The molecular docking study was performed to evaluate the binding affinity and interaction profile of selected phytoconstituents from *Cissus verticillata* against DPP-IV (PDB ID: 1X70) (Table 2). The docking results were compared with the native ligand (NL-1X70), which exhibited a docking score of −9.0 kcal/mol with key hydrogen bond interactions involving GLU205 and GLU206, along with hydrophobic interactions with residues such as TYR662, PHE357, and TYR666. These residues are known to play a critical role in the active site of DPP-IV, indicating the validity of the docking protocol.

Among the tested compounds, stigmasterol showed the highest binding affinity with a docking score of −9.6 kcal/mol, followed by campesterol (−9.4 kcal/mol) and pentanoic acid, 3-methyl-4-oxo (−9.3 kcal/mol). These values were comparable to or better than the native ligand, suggesting strong inhibitory potential. Stigmasterol and campesterol primarily exhibited hydrophobic interactions, particularly with key residues such as PHE357, TYR662, TYR666, and HIS740, forming stable complexes within the binding pocket. Similarly, γ-sitosterol also demonstrated a high docking score (−9.2 kcal/mol) with dominant hydrophobic interactions, further supporting the importance of sterol-based compounds in enzyme inhibition.

Benzoic acid, 3,4,5-trihydroxy-, methyl ester showed a significant docking score of −8.0 kcal/mol and formed multiple conventional hydrogen bonds with residues such as ASP739, GLU205, ASP709, ARG125, and ASN710. The presence of multiple hydrogen bonds suggests strong binding stability and specificity within the active site.

Moderate binding affinities were observed for compounds such as 2-methoxy-4-vinylphenol (−6.0 kcal/mol), 3,7,11,15-tetramethyl-2-hexadecen-1-ol (−6.0 kcal/mol), phenol derivatives (−6.1 kcal/mol), and neophytadiene (−5.9 kcal/mol), which primarily interacted through hydrophobic and π-based interactions. In contrast, lower docking scores were recorded for fatty acids such as n-hexadecanoic acid (−5.1 kcal/mol) and tetradecanoic acid (−5.6 kcal/mol), indicating comparatively weaker binding interactions. Notably, 1,2,3-benzenetriol (−5.6 kcal/mol) formed hydrogen bonds with GLU205 and ASN710, highlighting the role of polar interactions in ligand binding, although its overall binding affinity was lower than sterol compounds. Similarly, 9,12-octadecadienoic acid methyl ester (−5.5 kcal/mol) showed limited hydrogen bonding and hydrophobic interactions. Overall, the docking results indicate that phytosterols (stigmasterol, campesterol, and γ-sitosterol) and certain phenolic derivatives exhibit strong binding affinity toward DPP-IV, primarily through hydrophobic interactions and hydrogen bonding with key active site residues such as GLU205, PHE357, TYR662, and HIS740. These findings suggest that *Cissus verticillata* contains bioactive compounds with significant potential as DPP-IV inhibitors, supporting its possible role in the management of diabetes.

Table 2: Molecular docking interactions of selected phytoconstituents with DPP-IV enzyme, including binding residues, interaction types, ligand energy, and docking scores

Amino Acid	Bond Length	Bond Type	Bond Category	Ligand Energy (Kcal/mol)	Docking Score
NL_1X70					
GLU205	2.06051	Hydrogen Bond	Conventional Hydrogen Bond	428.59	-9
GLU206	2.63201				
GLU205	2.74228				
VAL207	3.10459	Halogen	Halogen (Fluorine)		
SER630	3.24455				
TYR662	5.12047	Hydrophobic	Pi-Pi Stacked		
PHE357	4.23194				
TYR666	4.04817		Pi-Alkyl		
1,2,3-Benzenetriol					
GLU205	2.48623	Hydrogen Bond	Conventional Hydrogen Bond	49.61	-5.6
ASN710	1.87804				
ARG125	4.52807	Hydrophobic	Pi-Alkyl		
2-Methoxy-4-vinylphenol					
SER630	3.46758	Hydrogen Bond	Carbon Hydrogen Bond	81.23	-6
TYR662	5.30506	Hydrophobic	Pi-Pi Stacked		
TYR666	5.04867		Pi-Pi T-shaped		
VAL656	4.60973		Alkyl		
TYR631	5.10516		Pi-Alkyl		
TRP659	4.85302				
TYR662	4.12426				
TYR666	4.40279				
3,7,11,15-Tetramethyl-2-hexadecen-1-ol					
TYR662	3.97341	Hydrophobic	Pi-Sigma	250.35	-6
VAL656	5.40349		Alkyl		
VAL711	4.73449				
VAL656	4.66468				
PHE357	4.59695		Pi-Alkyl		
TYR631	5.20344				
TRP659	4.79207				
TYR662	4.3963				
TYR666	4.22996				
HIS740	5.23939				
9,12-Octadecadienoic acid, methyl ester					
ARG429	2.54672	Hydrogen Bond	Conventional Hydrogen Bond	11.81	-5.5
TYR585	2.55463				
VAL656	4.67218	Hydrophobic	Alkyl		
TYR631	5.32667		Pi-Alkyl		
TRP659	5.14779				
TYR662	4.05477				
TYR666	4.55386				

Benzoic acid, 3,4,5-trihydroxy-, methyl ester					
ASP739	1.92315	Hydrogen Bond	Conventional Hydrogen Bond	65.35	-8
GLU205	2.01145				
ASP709	1.85836				
ARG125	2.69681				
ASN710	1.77117				
HIS740	3.71399		Carbon Hydrogen Bond		
ARG125	4.36255	Hydrophobic	Pi-Alkyl		
Campesterol					
PHE357	3.58848	Hydrophobic	Pi-Sigma	411.45	-9.4
TYR666	3.9468				
TYR666	3.91924				
PHE357	5.04794		Pi-Alkyl		
PHE357	4.81544				
PHE357	4.5484				
TYR662	5.1636				
TYR662	4.2598				
TYR662	5.26973				
HIS740	5.02647				
Gamma_Sitosterol					
PHE357	3.60106	Hydrophobic	Pi-Sigma	425.72	-9.2
TYR666	3.84464				
VAL711	4.80167		Alkyl		
PHE357	5.09393		Pi-Alkyl		
PHE357	4.85773				
PHE357	4.53104				
TYR662	4.53331				
TYR662	4.48727				
TYR666	5.35838				
HIS740	4.95553				
HIS740	5.15992				
Neophytadiene					
VAL711	4.73342	Hydrophobic	Alkyl	47.06	-5.9
VAL656	4.68725				
PHE357	5.32444		Pi-Alkyl		
PHE357	4.73975				
PHE357	4.8896				
TYR547	5.23726				
TYR631	5.18665				
TRP659	4.85138				
TYR662	4.57258				
TYR662	4.01923				
TYR666	4.26332				
HIS740	4.79659				
n-Hexadecanoic acid					

VAL207	2.41487	Hydrogen Bond	Conventional Hydrogen Bond	2.1	-5.1
ARG358	2.17698				
PHE357	3.56887	Hydrophobic	Pi-Sigma		
VAL656	4.72011		Alkyl		
TYR631	4.98283		Pi-Alkyl		
TRP659	4.96466				
TYR662	4.30803				
TYR666	4.42687				
Pentanoic acid, 3-methyl-4-oxo					
GLU205	3.62059	Electrostatic	Attractive Charge	355.51	-9.3
GLU206	4.7362				
HIS740	2.4183	Hydrogen Bond	Conventional Hydrogen Bond		
ARG125	2.80488				
ARG125	2.10651				
ARG358	2.6783				
ASN710O	2.76248				
GLU206	3.88366	Electrostatic	Pi-Anion		
HIS740	2.92036	Hydrogen Bond	Pi-Donor Hydrogen Bond		
PHE357	4.51051	Hydrophobic	Pi-Pi Stacked		
PHE357	4.56363		Pi-Alkyl		
Phenol, 3,5-bis(1,1-dimethylethyl)					
GLU205	2.35139	Hydrogen Bond	Conventional Hydrogen Bond	137.67	-6.1
GLU206	2.34067				
PHE357	3.78288	Hydrophobic	Pi-Pi Stacked		
PHE357	4.44487		Pi-Alkyl		
Stigmasterol					
PHE357	3.58537	Hydrophobic	Pi-Sigma	422.43	-9.6
VAL711	5.03301		Alkyl		
PHE357	4.97567		Pi-Alkyl		
PHE357	4.81797				
PHE357	4.52017				
TYR547	5.35197				
TYR662	4.48959				
TYR662	4.63517				
TYR666	5.43317				
TYR666	3.67321				
HIS740	5.00411				
HIS740	4.64424				
Tetradecanoic acid					
VAL207	2.62637	Hydrogen Bond	Conventional Hydrogen Bond	3.05	-5.6
ARG358	2.57229				
TYR662	3.9822	Hydrophobic	Pi-Sigma		
VAL656	4.60772		Alkyl		
TYR631	5.22717		Pi-Alkyl		
TRP659	4.84415				
TYR666	4.34802				

Table 3: Two-dimensional (2D) and three-dimensional (3D) binding interaction profiles of selected compounds with DPP-IV compared to the native ligand

3D Binding Interaction	2D Binding Interaction
NL_1X70	
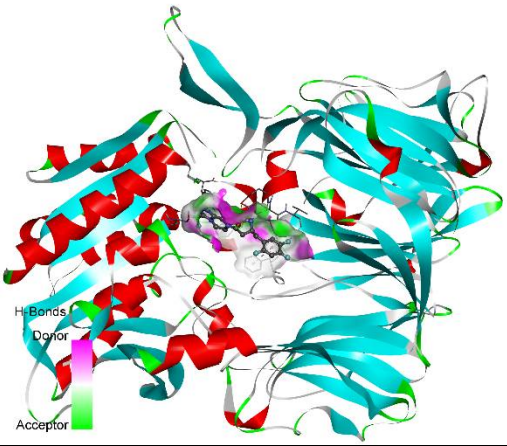	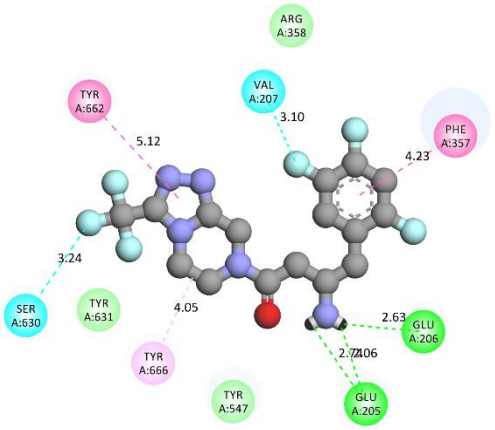
1,2,3-Benzenetriol	
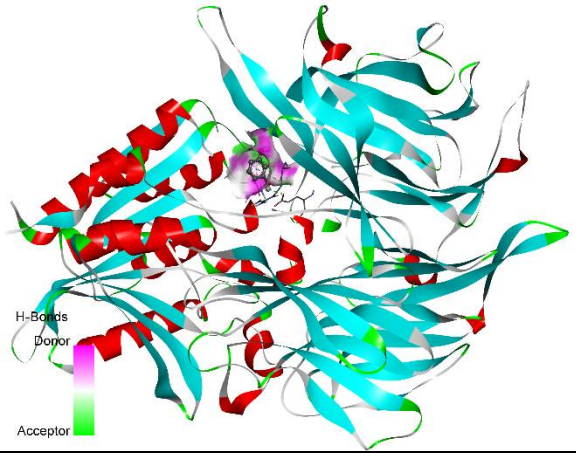	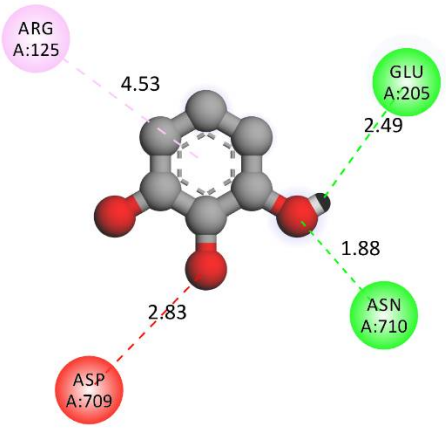
2-Methoxy-4-vinylphenol	
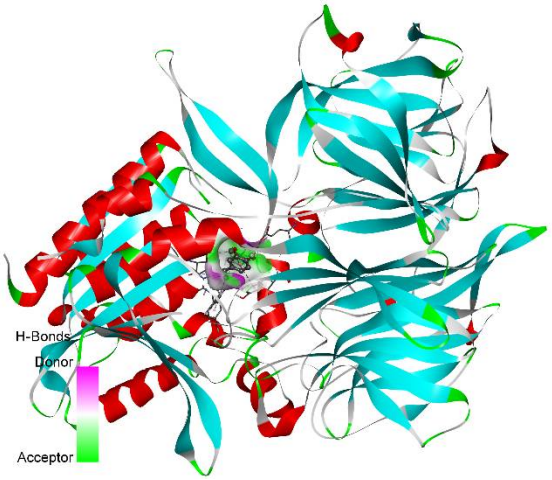	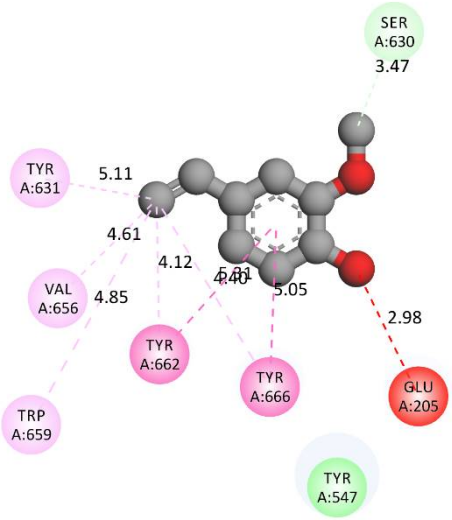
3,7,11,15-Tetramethyl-2-hexadecen-1-ol	

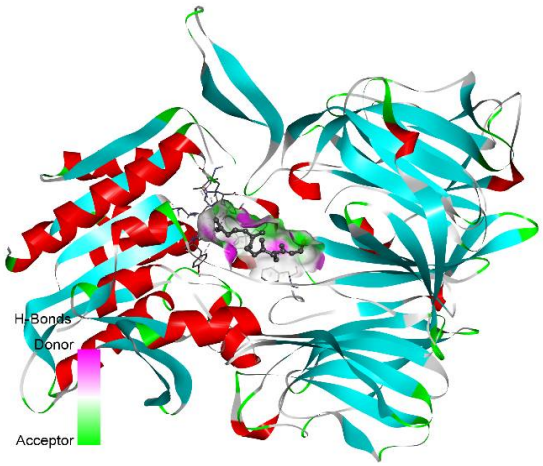	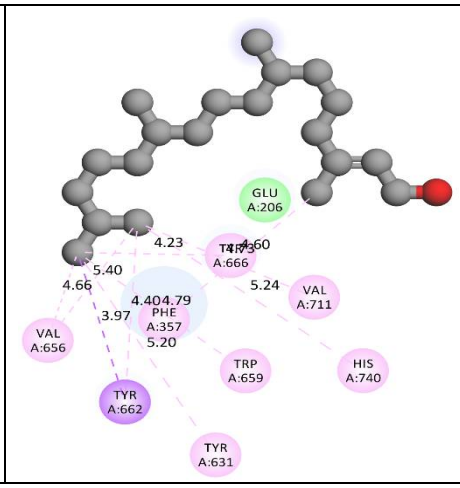
9,12-Octadecadienoic acid, methyl ester	
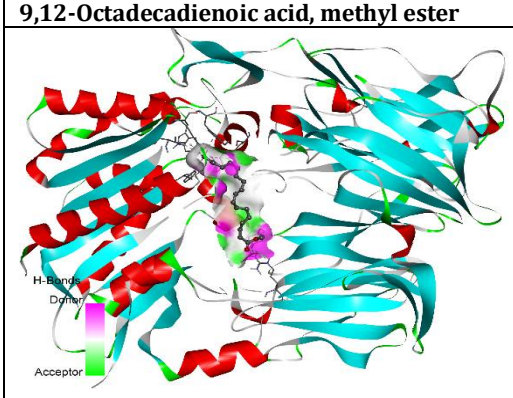	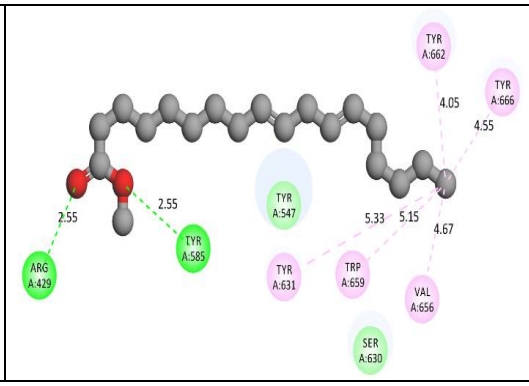
Benzoic acid, 3,4,5-trihydroxy-, methyl ester	
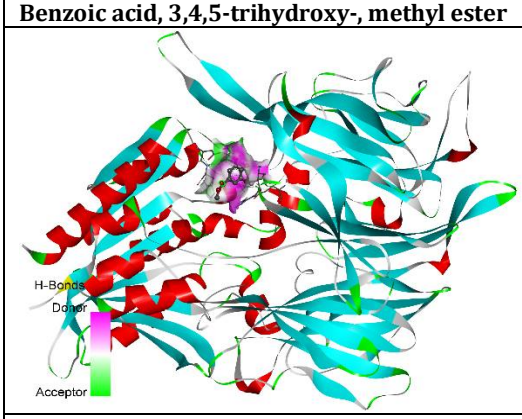	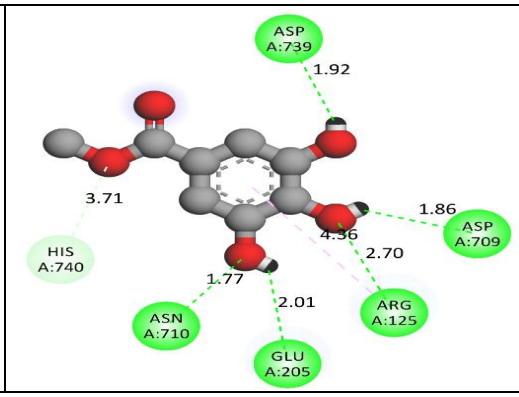
Campesterol	
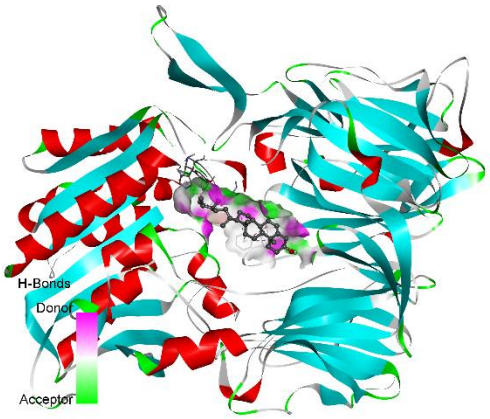	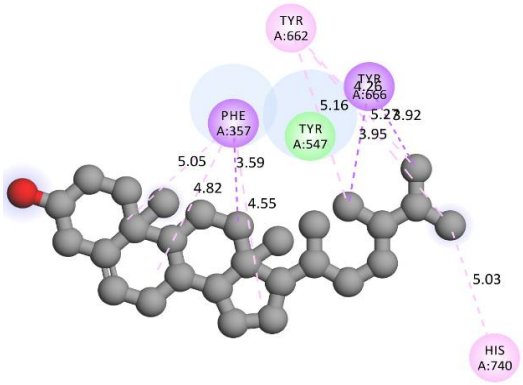
Gamma_Sitosterol	

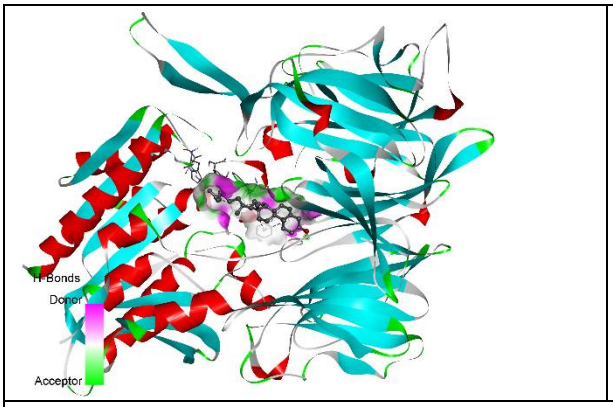

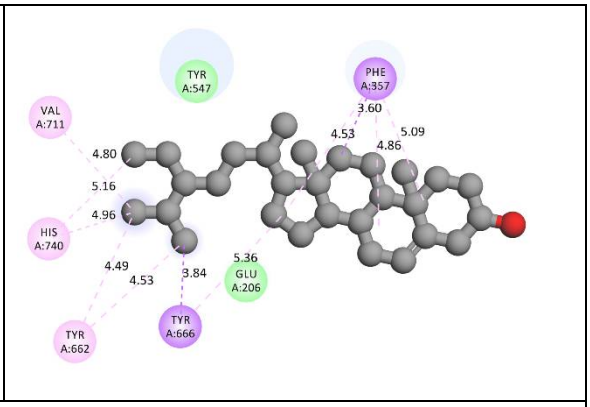

Neophytadiene

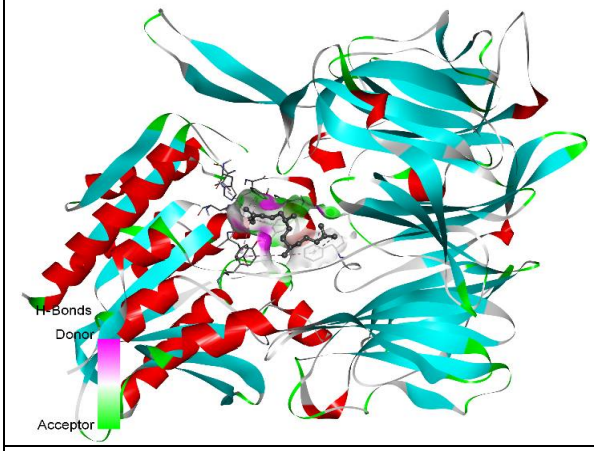

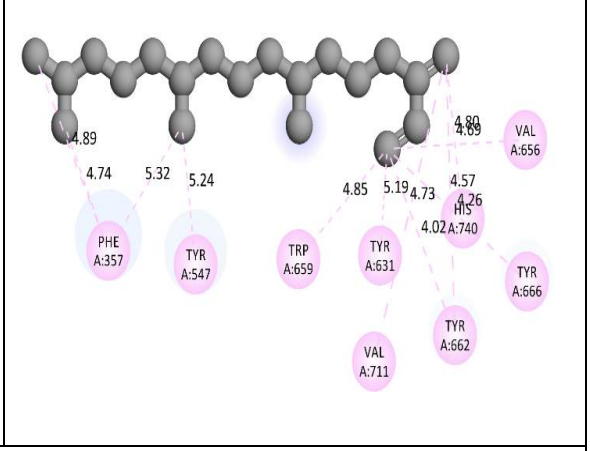

n-Hexadecanoic acid

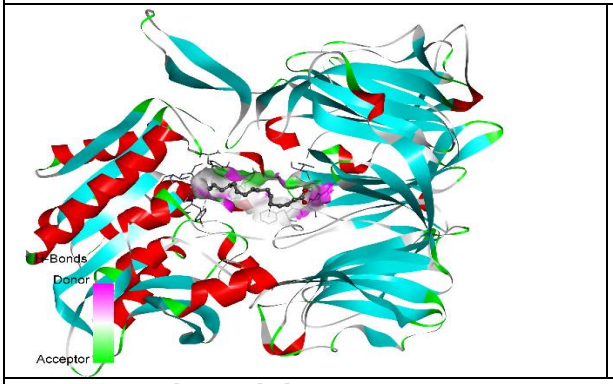

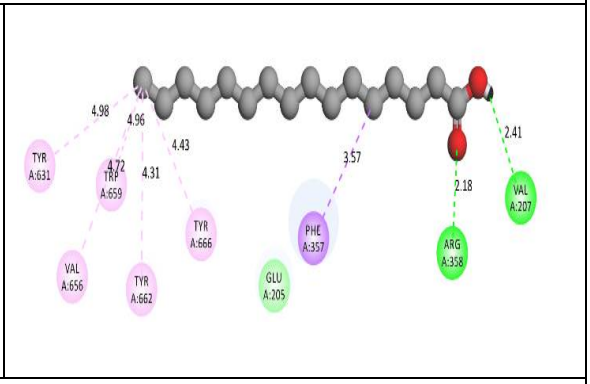

Pentanoic acid, 3-methyl-4-oxo

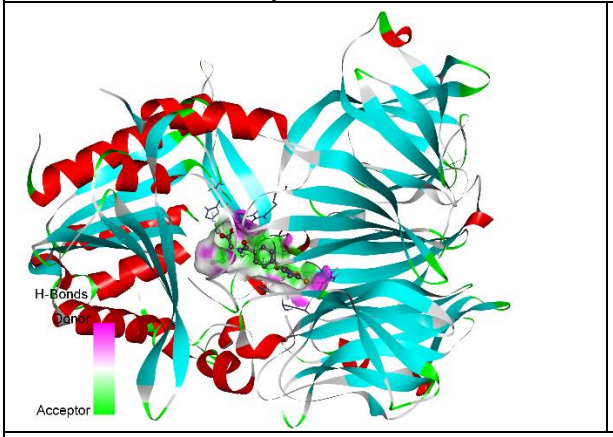

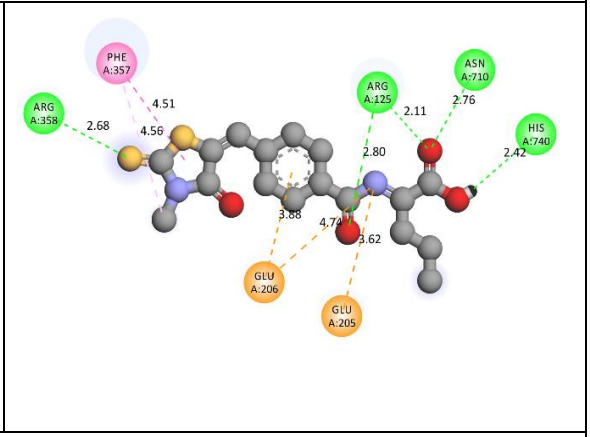

Phenol, 3,5-bis(1,1-dimethylethyl)

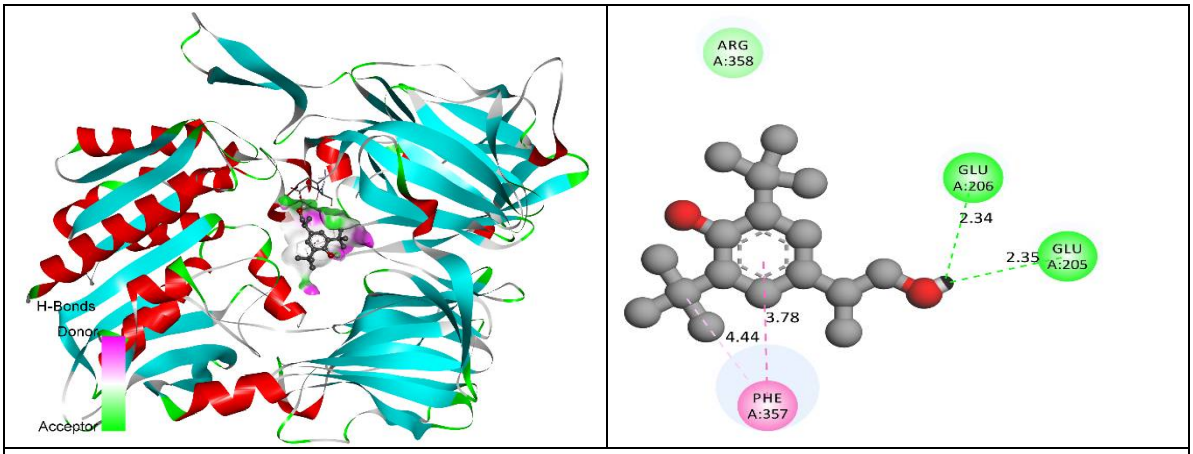

Stigmasterol

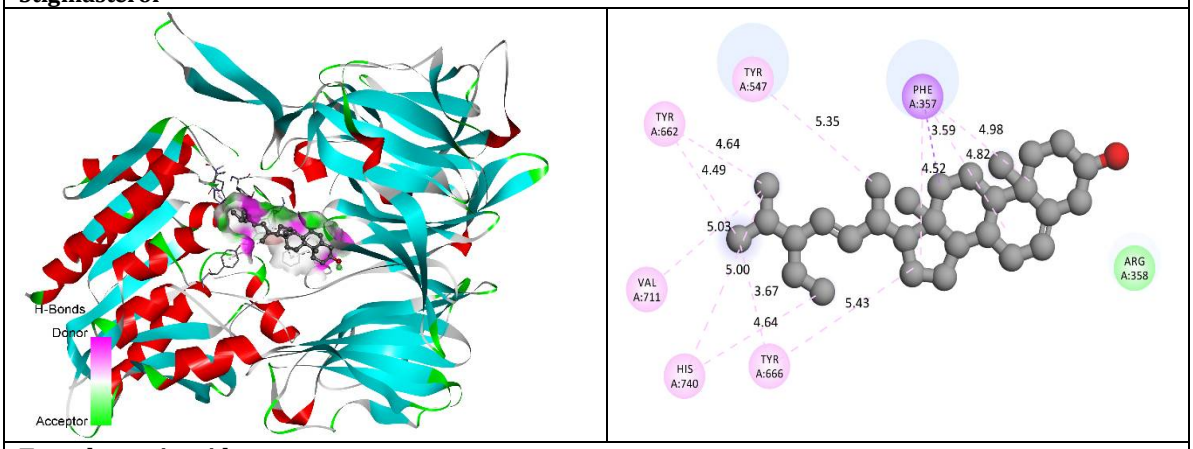

Tetradecanoic acid

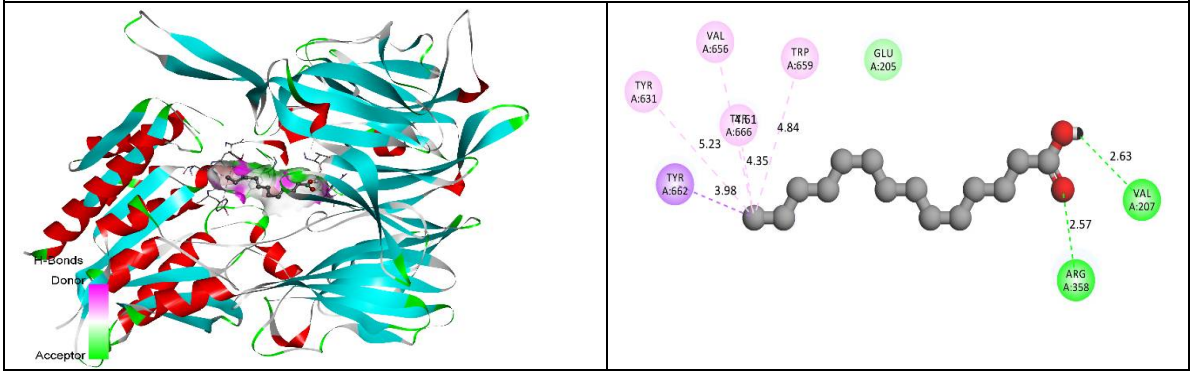

ADMET Analysis

The physicochemical and ADMET properties of selected phytoconstituents from *Cissus verticillata* were evaluated to determine their drug-likeness and pharmacokinetic suitability (Table 4). The native ligand (NL-1X70) showed balanced properties with molecular weight (407.12 g/mol), TPSA (77.04 Å^2), logP (1.38), and moderate solubility (logS −3.01), serving as a standard reference. Among the tested compounds, 1,2,3-benzenetriol (MW 126.03 g/mol, TPSA 60.69 Å^2, logP 0.84, logS 0.45) and benzoic acid, 3,4,5-trihydroxy-, methyl ester (MW 184.04 g/mol, TPSA 86.99 Å^2, logP 1.05, logS −1.79) exhibited favorable polarity, hydrogen bonding capacity (nHD = 3, nHA = 5), and good solubility, indicating strong absorption potential. Similarly, 2-methoxy-4-vinylphenol (MW 150.07 g/mol, TPSA 29.46 Å^2, logP 2.05) showed moderate lipophilicity and acceptable solubility (logS −1.63), supporting its drug-like behavior.

In contrast, phytosterols such as campesterol (MW 400.37 g/mol, logP 7.66), γ-sitosterol (MW 414.39 g/mol, logP 7.84), and stigmasterol (MW 412.37 g/mol, logP 6.57) demonstrated high lipophilicity with low TPSA (~20.23 Å^2) and poor solubility (logS < −5.7), suggesting strong membrane permeability but limited aqueous solubility. Similarly, long-chain compounds including neophytadiene (logP 7.97, logS −7.95), 3,7,11,15-tetramethyl-2-hexadecen-1-ol (logP 7.57), and 9,12-octadecadienoic acid methyl ester

(logP 7.01) exhibited high hydrophobicity and low polarity, which may reduce bioavailability despite favorable membrane interaction.

Fatty acids such as n-hexadecanoic acid (MW 256.24 g/mol, TPSA 37.3 Å^2, logP 6.64) and tetradecanoic acid (MW 228.21 g/mol, logP 5.72) showed moderate lipophilicity with acceptable hydrogen bonding (nHD = 1–2), indicating moderate pharmacokinetic behavior. Pentanoic acid, 3-methyl-4-oxo (MW 378.07 g/mol, TPSA 86.71 Å^2, logP 1.09) displayed balanced polarity and solubility (logS −3.18), similar to the native ligand. Overall, the ADMET results indicate that phenolic and ester compounds possess better solubility and polarity, while sterols and terpenoids exhibit high lipophilicity and permeability. These findings suggest that compounds with balanced physicochemical properties, particularly benzenetriol and phenolic esters, may serve as promising DPP-IV inhibitors with favorable pharmacokinetic profiles.

Table 4: Physicochemical properties of selected compounds including molecular weight, polarity (TPSA), solubility (logS), lipophilicity (logP), and structural descriptors

Compounds	MW	Volume	Dense	nHA	nHD	nRot	nRing	TPSA	logS	logP
NL-1X70	407.12	343.9835	1.183545	6	2	6	3	77.04	-3.01445	1.38032
1,2,3-Benzenetriol	126.03	122.2372	1.031028	3	3	0	1	60.69	0.456817	0.849219
2-Methoxy-4-vinylphenol	150.07	162.6985	0.922381	2	1	2	1	29.46	-1.63923	2.052078
3,7,11,15-Tetramethyl-2-hexadecen-1-ol	296.31	360.6299	0.821646	1	1	13	0	20.23	-6.40616	7.574417
9,12-Octadecadienoic acid, methyl ester	294.26	346.8513	0.848375	2	0	15	0	26.3	-6.57696	7.012045
Benzoic acid, 3,4,5-trihydroxy-, methyl ester	184.04	171.7732	1.071413	5	3	2	1	86.99	-1.79671	1.053127
Campesterol	400.37	464.772	0.861433	1	1	5	4	20.23	-6.92787	7.662918
Gamma_Sitosterol	414.39	482.068	0.859609	1	1	6	4	20.23	-6.95394	7.845348
Neophytadiene	278.3	349.2032	0.796957	0	0	13	0	0	-7.95449	7.979378
n-Hexadecanoic acid	256.24	300.2362	0.853461	2	1	14	0	37.3	-5.69319	6.647652
Pentanoic acid, 3-methyl-4-oxo	378.07	358.5561	1.054424	6	2	7	2	86.71	-3.18892	1.090174
Phenol, 3,5-bis(1,1-dimethylethyl)	264.21	303.7028	0.869962	2	2	4	1	40.46	-4.16851	4.295893
Stigmasterol	412.37	479.4315	0.860123	1	1	5	4	20.23	-5.73287	6.570423
Tetradecanoic acid	228.21	265.6442	0.859081	2	1	12	0	37.3	-4.87761	5.723228

The drug-likeness properties of selected phytoconstituents from *Cissus verticillata* were evaluated using QED, NP score, and multiple rule-based filters (Table 5). The native ligand (NL-1X70) exhibited a QED value of 0.622 and NP score of −1.404, indicating moderate drug-likeness with acceptable compliance to GSK rule (1) but not Golden Triangle or Chelator rules.

Among the compounds, phenol, 3,5-bis(1,1-dimethylethyl) showed the highest QED value (0.845) with NP score of 0.525, indicating excellent drug-likeness, although it violated Pfizer and GSK rules. Similarly, 2-methoxy-4-vinylphenol demonstrated a high QED (0.699) and NP score (1.011), satisfying Golden Triangle and Chelator rules, suggesting an optimal balance of solubility and permeability. 1,2,3-benzenetriol (QED 0.45, NP score 0.798) and benzoic acid, 3,4,5-trihydroxy-, methyl ester (QED 0.439, NP score 0.711) also complied with Golden Triangle and Chelator rules, indicating favorable pharmacokinetic profiles. Phytosterols such as stigmasterol (QED 0.457, NP score 2.802), γ-sitosterol (QED 0.436, NP score 2.681), and campesterol (QED 0.47, NP score 2.676) exhibited high NP scores, confirming strong natural origin, but violated Pfizer and GSK rules, indicating possible limitations in toxicity or bioavailability despite satisfying Golden Triangle (campesterol and γ-sitosterol). Long-chain compounds such as 3,7,11,15-tetramethyl-2-hexadecen-1-ol (QED 0.392, NP score 1.532), 9,12-octadecadienoic acid methyl ester (QED 0.224, NP score 1.03), neophytadiene (QED 0.313, NP score 1.365), n-hexadecanoic acid (QED 0.413, NP score 0.385), and tetradecanoic acid (QED 0.488, NP score 0.433) showed lower QED values and violated Pfizer and GSK rules, reflecting reduced drug-likeness and pharmacokinetic limitations. Pentanoic acid, 3-methyl-4-oxo displayed moderate drug-likeness (QED 0.584, NP score −1.194) with no rule violations but did not satisfy Golden Triangle or Chelator criteria. Overall, phenolic compounds

demonstrated better drug-likeness, rule compliance, and balanced pharmacokinetic properties, whereas sterols and long-chain hydrocarbons exhibited strong natural origin but limited drug-likeness. These results suggest that phenolic derivatives are more promising candidates for further development as DPP-IV inhibitors.

Table 5: Drug-likeness evaluation of selected compounds based on QED, natural product score, and rule-based filters (Lipinski, Pfizer, GSK, Golden Triangle, Chelator)

Compounds	**QED**	**NP Score**	**Lipinski rule**	**Pfizer Rule**	**GSK Rule**	**Golden Triangle**	**Chelator Rule**
NL-1X70	0.622	-1.404	0	0	1	0	0
1,2,3-Benzenetriol	0.45	0.798	0	0	0	1	1
2-Methoxy-4-vinylphenol	0.699	1.011	0	0	0	1	1
3,7,11,15-Tetramethyl-2-hexadecen-1-ol	0.392	1.532	0	1	1	0	0
9,12-Octadecadienoic acid, methyl ester	0.224	1.03	0	1	1	0	0
Benzoic acid, 3,4,5-trihydroxy-, methyl ester	0.439	0.711	0	0	0	1	1
Campesterol	0.47	2.676	0	1	1	1	0
Gamma_Sitosterol	0.436	2.681	0	1	1	1	0
Neophytadiene	0.313	1.365	0	1	1	0	0
n-Hexadecanoic acid	0.413	0.385	0	1	1	0	0
Pentanoic acid, 3-methyl-4-oxo	0.584	-1.194	0	0	0	0	0
Phenol, 3,5-bis(1,1-dimethylethyl)	0.845	0.525	0	1	1	0	0
Stigmasterol	0.457	2.802	0	1	1	0	0
Tetradecanoic acid	0.488	0.433	0	1	1	0	0

The absorption properties of selected phytoconstituents from *Cissus verticillata* were evaluated using parameters such as Caco-2 permeability, MDCK permeability, P-glycoprotein (Pgp) interaction, human intestinal absorption (HIA), and oral bioavailability indices (Table 6). The native ligand (NL-1X70) showed low permeability values (Caco-2: −5.148, MDCK: −4.696) and negligible HIA (0), indicating limited intestinal absorption despite high Pgp-substrate probability (0.992). Among the tested compounds, 1,2,3-benzenetriol exhibited relatively better absorption with Caco-2 permeability (−4.926), HIA (0.105), and high oral bioavailability (F50% = 0.943). Similarly, 2-methoxy-4-vinylphenol showed moderate permeability (−4.806), with improved bioavailability (F50% = 0.911) and low Pgp interaction, suggesting favorable absorption characteristics.

Benzoic acid, 3,4,5-trihydroxy-, methyl ester demonstrated lower permeability (−5.433) but high oral bioavailability (F50% = 0.990), indicating that despite limited permeability, it may achieve significant systemic availability. Pentanoic acid, 3-methyl-4-oxo also showed moderate HIA (0.198) and high bioavailability (F50% = 0.998), supporting its absorption potential. Fatty acids such as n-hexadecanoic acid (HIA = 0.849) and tetradecanoic acid (HIA = 0.756) exhibited high intestinal absorption, although their bioavailability at higher thresholds (F50%) was relatively lower (0.438 and 0.327, respectively). In contrast, phytosterols such as campesterol, γ-sitosterol, and stigmasterol showed very low HIA values ($\sim 10^{-6}$), indicating poor intestinal absorption despite moderate permeability and high F50% values (>0.96). This suggests that their high lipophilicity may limit effective absorption. Neophytadiene and long-chain terpenoids displayed low HIA but high F50% values (>0.99), indicating potential bioavailability limitations due to poor absorption. Phenol, 3,5-bis(1,1-dimethylethyl) showed strong Pgp inhibition (0.919) and high bioavailability (F50% = 0.998), suggesting possible drug–transporter interactions. Overall, phenolic compounds and small molecules demonstrated better absorption profiles with balanced permeability and bioavailability, whereas sterols and long-chain hydrophobic compounds exhibited poor intestinal absorption. These findings indicate that compounds such as 1,2,3-benzenetriol, 2-methoxy-4-vinylphenol, and pentanoic acid derivatives possess favorable absorption characteristics for potential DPP-IV inhibition.

Table 6: Predicted absorption parameters of selected compounds including permeability (Caco-2, MDCK), P-glycoprotein interaction, human intestinal absorption, and oral bioavailability indices

Compounds	Caco-2 Permeability	MDCK Permeability	Pgp-inhibitor	Pgp-substrate	HIA	F20%	F30%	F50%
NL-1X70	-5.14825	-4.69623	0.000759	0.992536	0	0.000283	1.26E-05	1.63E-05
1,2,3-Benzenetriol	-4.92626	-4.75442	0.004659	0.042992	0.105284	0.845857	0.901101	0.943925
2-Methoxy-4-vinylphenol	-4.80684	-4.75253	0.34643	0.066965	0.094682	0.714982	0.620571	0.911944
3,7,11,15-Tetramethyl-2-hexadecen-1-ol	-4.9629	-4.77246	0.001474	8.60E-05	0.018995	0.003992	0.656773	0.967339
9,12-Octadecadienoic acid, methyl ester	-4.99874	-4.72111	0.626031	0.00362	0.001123	0.251378	0.377595	0.924807
Benzoic acid, 3,4,5-trihydroxy-, methyl ester	-5.43349	-4.83148	0.021275	0.01834	0.000622	0.831758	0.864436	0.990609
Campesterol	-5.15495	-5.04813	0.000675	0.324287	4.77E-07	0.005395	0.190669	0.985724
Gamma_Sitosterol	-5.21088	-4.99484	0.000193	0.078368	1.07E-06	0.002384	0.137875	0.987736
Neophytadiene	-4.97407	-4.76042	0.000934	0.000943	0.000551	0.028382	0.898467	0.995524
n-Hexadecanoic acid	-5.09587	-4.80282	2.06E-05	0.014421	0.849536	0.738221	0.925655	0.438166
Pentanoic acid, 3-methyl-4-oxo	-5.08278	-4.85403	0.096426	1.61E-07	0.198504	0.369677	0.904156	0.998289
Phenol, 3,5-bis(1,1-dimethylethyl)	-4.9746	-4.82992	0.919348	0.715923	0.192531	0.973393	0.923698	0.998459
Stigmasterol	-5.25627	-4.92488	0.049433	0.020969	9.54E-07	0.008377	0.173348	0.963939
Tetradecanoic acid	-5.09766	-4.78904	3.58E-05	0.018977	0.756654	0.604258	0.837822	0.32716

The distribution and metabolism profiles of selected phytoconstituents from *Cissus verticillata* were evaluated based on plasma protein binding (PPB%), volume of distribution (VD), blood–brain barrier (BBB) permeability, fraction unbound (Fu), and cytochrome P450 (CYP) enzyme interactions (Table 7). The native ligand (NL-1X70) showed moderate PPB (58.00%) and VD (0.58), with very low BBB permeability (8.38E−06), indicating limited central nervous system penetration. Among the compounds, phytosterols such as stigmasterol (98.64%), γ-sitosterol (86.31%), and campesterol (83.28%) exhibited high PPB values, suggesting strong plasma protein binding and prolonged systemic retention. However, their low BBB permeability (≤0.066) indicates restricted brain distribution. Similarly, fatty acid derivatives such as n-hexadecanoic acid (98.03%) and tetradecanoic acid (97.44%) also showed high PPB with moderate VD (~0.4–0.59), indicating efficient systemic distribution.

Phenolic compounds such as 1,2,3-benzenetriol (PPB 56.54%, VD −0.32) and benzoic acid derivative (PPB 60.00%, VD −0.43) showed lower protein binding and negative VD values, suggesting limited tissue distribution but higher free fraction availability (Fu ~33–34%). Notably, neophytadiene demonstrated high BBB permeability (0.973), indicating potential central nervous system penetration, unlike most other compounds.

Metabolism analysis revealed that several compounds interact with CYP enzymes. 2-methoxy-4-vinylphenol showed strong inhibition of CYP1A2 (0.989) and CYP3A4 (0.892), indicating possible drug–drug interaction risks. Similarly, fatty acid ester (9,12-octadecadienoic acid methyl ester) showed strong inhibition across multiple CYP isoforms (CYP1A2, CYP2C19, CYP2C9, CYP3A4 ~0.93–0.99), suggesting metabolic interference. In contrast, compounds such as 1,2,3-benzenetriol and benzoic acid derivatives showed moderate CYP interactions with relatively lower inhibition probabilities, indicating safer metabolic profiles. Phytosterols primarily acted as CYP3A4 substrates (campesterol 0.989, γ-sitosterol 0.999, stigmasterol 0.995), suggesting metabolism via this pathway.

Overall, sterols and fatty acids demonstrated high plasma binding and systemic distribution but limited BBB penetration, whereas phenolic compounds exhibited better free fraction and safer metabolic profiles. These findings indicate that phenolic derivatives possess more favorable distribution and metabolism characteristics for development as DPP-IV inhibitors.

Table 7: Distribution and metabolism profiles of selected compounds including plasma protein binding, volume of distribution, BBB permeability, and CYP450 enzyme interactions

Compounds	Distribution				Metabolism									
					CYP1A2		CYP2C19		CYP2C9		CYP2D6		CYP3A4	
	PPB%	VD	BBB	Fu	Inhibitor	Substrate	Inhibitor	Substrate	Inhibitor	Substrate	Inhibitor	Substrate	Inhibitor	Substrate
NL-1X70	58.0064	0.584768	8.38E-06	39.35685	1.18E-05	0.139781	0.000417	0.94269	9.71E-07	9.66E-05	0.001282	0.003987	0.000232	0.756225
1,2,3-Benzenetriol	56.54544	-0.32581	0.549543	34.51515	0.29901	0.021303	0.000419	0.000745	0.001304	0.735433	4.13E-05	0.946613	0.197083	0.000633
2-Methoxy-4-vinylphenol	86.32645	-0.40505	0.066267	12.73905	0.989206	0.46211	0.300878	0.792644	0.103082	0.608688	0.09797	0.947399	0.892514	0.002264
3,7,11,15-Tetramethyl-2-hexadecen-1-ol	84.71563	0.071956	0.607761	13.82408	0.000157	0.002335	0.326897	0.99007	0.995605	0.995801	0.399953	0.357824	0.358333	0.00864
9,12-Octadecadienoic acid, methyl ester	98.12085	-0.30672	0.005116	1.351312	0.999964	7.69E-06	0.999954	0.023234	0.93313	0.999979	0.019918	0.999495	0.999575	1.35E-07
Benzoic acid, 3,4,5-trihydroxy-, methyl ester	60.0063	-0.43168	0.029786	33.47891	0.690646	0.017017	0.217697	0.000209	0.85209	0.10053	0.000179	0.123663	0.904037	7.50E-06
Campesterol	83.28198	-0.16791	0.066315	15.48761	1.68E-06	1.82E-08	0.001562	0.003897	0.122845	9.22E-07	0.071877	0.009077	0.184067	0.989626
Gamma_Sitosterol	86.31003	-0.10081	0.059511	14.37152	3.06E-07	8.15E-07	8.51E-05	0.287484	0.102538	7.51E-07	0.225381	0.03554	0.075418	0.999903
Neophytadiene	98.12719	0.57914	0.973867	1.523978	0.00505	0.004255	0.997867	0.996767	0.999758	0.993176	0.6705	0.182822	0.383352	0.009973
n-Hexadecanoic acid	98.03125	0.592197	0.020998	1.671825	0.072816	8.23E-05	0.015061	0.061985	0.165551	0.99999	0.146891	0.732832	1.25E-05	5.50E-05
Pentanoic acid, 3-methyl-4-oxo	97.05022	-0.15451	0.09206	2.433584	6.93E-05	1.12E-05	0.733609	9.75E-11	0.981409	0.000554	2.81E-07	6.51E-05	2.25E-06	5.51E-06
Phenol, 3,5-bis (1,1-dimethylethyl)	94.50026	0.206952	0.016414	4.248336	0.114344	5.46E-06	0.309186	0.057384	0.091933	0.000193	0.031788	0.000394	0.020513	0.819143

Stigmasterol	98.64921	-0.10121	0.000528	0.956151	2.80E-06	2.39E-11	0.000554	2.32E-07	0.000339	1.16E-09	0.009694	0.002692	0.059435	0.995375
Tetradecanoic acid	97.44871	0.418707	0.035986	2.108519	0.071367	7.71E-05	0.014434	0.060129	0.16592	0.999988	0.14053	0.712885	1.24E-05	6.21E-05

The excretion and toxicity profiles of selected phytoconstituents from *Cissus verticillata* were evaluated using plasma clearance (CL-plasma), half-life (T1/2), and multiple toxicity endpoints (Table 8). The native ligand (NL-1X70) exhibited moderate clearance (6.51) and half-life (0.71), with high human hepatotoxicity (H-HT = 0.975) and respiratory toxicity (0.999), indicating potential safety concerns. Among the tested compounds, phenolic derivatives such as 1,2,3-benzenetriol (CL = 13.70; T1/2 = 1.69) and 2-methoxy-4-vinylphenol (CL = 10.32; T1/2 = 1.51) showed higher clearance and longer half-life, suggesting efficient elimination with sustained activity. However, these compounds exhibited moderate Ames toxicity (0.69 and 0.54) and high probabilities of eye irritation (>0.99).

Benzoic acid derivative (CL = 12.69; T1/2 = 1.60) also demonstrated favorable excretion but showed relatively higher DILI probability (0.627), indicating possible hepatotoxicity. Pentanoic acid, 3-methyl-4-oxo showed moderate clearance (3.67) and half-life (1.34) but an extremely high DILI value (0.999), suggesting significant liver toxicity risk. Phytosterols such as campesterol (CL = 14.51), γ-sitosterol (CL = 13.92), and stigmasterol (CL = 12.68) exhibited high clearance with moderate half-life (~0.55–0.69), indicating efficient systemic elimination. However, they showed higher carcinogenicity probabilities (0.75–0.87) and moderate toxicity risks, including skin sensitization (>0.94).

Fatty acids such as n-hexadecanoic acid and tetradecanoic acid showed lower clearance (~3.6–3.7) with moderate half-life (~0.80–0.93) and relatively low Ames toxicity (<0.07), suggesting better safety profiles compared to other compounds. Similarly, neophytadiene showed low half-life (0.15) and moderate toxicity parameters. Overall, phenolic compounds demonstrated better excretion profiles but moderate toxicity concerns, while sterols showed efficient clearance but higher carcinogenic and sensitization risks. Fatty acids exhibited comparatively safer toxicity profiles. These findings suggest that although several compounds show promising pharmacokinetics, toxicity parameters must be carefully considered in selecting potential DPP-IV inhibitors from *Cissus verticillata*.

Table 8: Excretion and toxicity profiles of selected compounds including clearance, half-life, hepatotoxicity, mutagenicity, and other safety parameters

Compounds	**Excretion**		**Toxicity**									
	CL-plasma	**T1/2**	**H-HT**	**DILI**	**Ames Toxicity**	**Rat Oral Acute Toxicity**	**FDAMDD**	**Skin Sensitization**	**Carcinogenicity**	**Eye Corrosion**	**Eye Irritation**	**Respiratory Toxicity**
NL-1X70	6.518834	0.714562	0.975344	0.621078	0.346963	0.994501	0.898177	0.987695	0.14283	4.18E-05	0.350347	0.999075
1,2,3-Benzenetriol	13.70077	1.696055	0.272355	0.394368	0.697564	0.456231	0.60608	0.999573	0.595589	0.981544	0.998922	0.691818
2-Methoxy-4-vinylphenol	10.32476	1.517637	0.350741	0.165793	0.546391	0.365064	0.210007	0.929057	0.594417	0.990839	0.997473	0.746635

3,7,11,15-Tetramethyl-2-hexadecen-1-ol	6.83429	0.325022	0.74688	0.018019	0.185981	0.03066	0.118087	0.99693	0.353182	0.967658	0.995708	0.816626
9,12-Octadecadienoic acid, methyl ester	5.900761	0.243798	0.143158	0.000319	0.185467	0.039654	0.045761	0.999951	0.051452	0.999478	0.997832	0.687781
Benzoic acid, 3,4,5-trihydroxy-, methyl ester	12.69368	1.602904	0.148041	0.627452	0.503833	0.203433	0.414563	0.996265	0.398039	0.455552	0.996422	0.279515
Campesterol	14.51213	0.695179	0.556978	0.250527	0.216314	0.143735	0.6133	0.946994	0.874873	0.499903	0.956759	0.798543
Gamma_Sitosterol	13.92719	0.614181	0.769177	0.135024	0.070547	0.104215	0.439884	0.993014	0.751685	0.736955	0.983853	0.394395
Neophytadiene	6.814592	0.159553	0.461108	0.013754	0.298852	0.162581	0.377001	0.995279	0.409832	0.999064	0.998621	0.827029
n-Hexadecanoic acid	3.770445	0.932167	0.422959	0.187545	0.04709	0.124449	0.178303	0.908553	0.269677	0.98317	0.997497	0.932895
Pentanoic acid, 3-methyl-4-oxo	3.674133	1.340398	0.585166	0.999999	0.12602	0.532644	0.313085	0.999965	0.482091	3.99E-06	0.235406	0.978512
Phenol, 3,5-bis(1,1-dimethylethyl)	7.9541	0.635933	0.424028	0.123704	0.115616	0.302156	0.506372	0.544847	0.286211	0.189794	0.964528	0.646418
Stigmasterol	12.68291	0.554144	0.573304	0.50829	0.158648	0.101031	0.731789	0.975274	0.874838	0.113305	0.953902	0.939648
Tetradecanoic acid	3.6228	0.807519	0.417041	0.198111	0.062635	0.133879	0.168436	0.859654	0.293324	0.983424	0.997437	0.90617

The environmental toxicity profile of selected phytoconstituents from *Cissus verticillata* was evaluated using parameters such as bioconcentration factor (BCF), IGC50 (protozoa toxicity), LC50 for fish (LC50FM), and LC50 for Daphnia magna (LC50DM) (Table 9) and (10). The native ligand (NL-1X70) showed moderate environmental impact with BCF (1.37), IGC50 (3.36), LC50FM (4.02), and LC50DM (4.85), serving as a reference for comparison. Among the tested compounds, phytosterols such as γ-sitosterol (BCF 3.28), campesterol (3.12), and stigmasterol (2.95) exhibited high BCF values, indicating a greater tendency for bioaccumulation in aquatic organisms. Similarly, neophytadiene (BCF 2.00) and phenol, 3,5-bis(1,1-dimethylethyl) (BCF 2.90) also showed relatively high accumulation potential.

Compounds such as 3,7,11,15-tetramethyl-2-hexadecen-1-ol demonstrated high toxicity values across parameters (IGC50 5.20, LC50FM 6.12, LC50DM 6.10), indicating comparatively lower environmental toxicity (higher LC50/IGC50 values reflect lower toxicity). Similarly, neophytadiene and sterols also

exhibited higher LC50 values (>5), suggesting reduced acute toxicity. In contrast, polar compounds such as benzoic acid, 3,4,5-trihydroxy-, methyl ester (BCF 0.54) and 2-methoxy-4-vinylphenol (BCF 0.89) showed lower bioaccumulation potential, indicating better environmental safety. Fatty acids such as n-hexadecanoic acid and tetradecanoic acid exhibited low LC50FM values (1.54 and 1.75), suggesting relatively higher toxicity toward aquatic organisms despite lower accumulation potential. Overall, sterols and hydrophobic compounds demonstrated higher bioaccumulation but lower acute toxicity, whereas polar phenolic compounds showed lower environmental persistence. These findings suggest that while *Cissus verticillata* contains compounds with favorable pharmacological properties, their environmental impact varies significantly and should be considered in drug development.

Table 9: Environmental toxicity assessment of selected compounds including bioconcentration factor (BCF), protozoal toxicity (IGC_{50}), and aquatic toxicity ($LC_{50}FM$, $LC_{50}DM$)

Compounds	**BCF**	**IGC50**	**LC50FM**	**LC50DM**
NL-1X70	1.378057	3.361339	4.028491	4.856742
1,2,3-Benzenetriol	1.258617	3.814048	4.014779	4.464336
2-Methoxy-4-vinylphenol	0.890793	3.140793	3.457028	4.075699
3,7,11,15-Tetramethyl-2-hexadecen-1-ol	2.600254	5.20097	6.128494	6.10525
9,12-Octadecadienoic acid, methyl ester	1.369483	4.495504	4.339975	5.893758
Benzoic acid, 3,4,5-trihydroxy-, methyl ester	0.541052	3.235442	3.904332	4.291835
Campesterol	3.125031	4.736946	5.429239	5.154125
Gamma_Sitosterol	3.286117	4.806799	5.579571	5.157156
Neophytadiene	2.005973	4.717852	5.933723	6.045163
n-Hexadecanoic acid	0.810951	3.830714	1.540689	5.495133
Pentanoic acid, 3-methyl-4-oxo	0.851034	3.818738	4.939875	5.306319
Phenol, 3,5-bis(1,1-dimethylethyl)	2.906152	3.741635	5.14818	5.634452
Stigmasterol	2.951101	4.532104	5.203026	5.204844
Tetradecanoic acid	0.924433	3.812916	1.753523	5.366167

Table 10: ADMET radar representation summarizing pharmacokinetic and drug-likeness properties of selected compounds compared with the native ligand

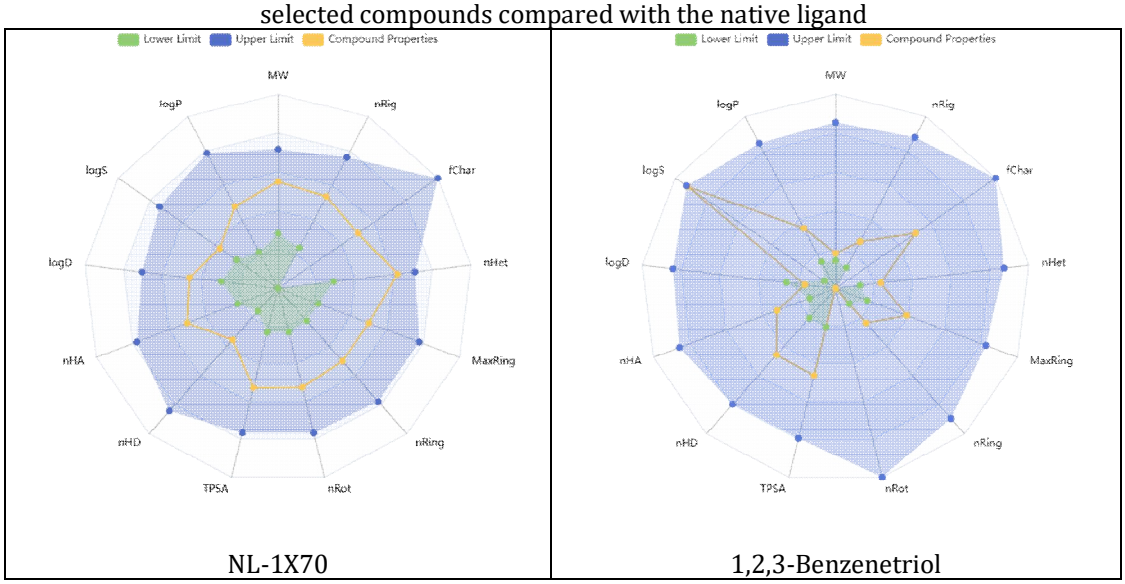

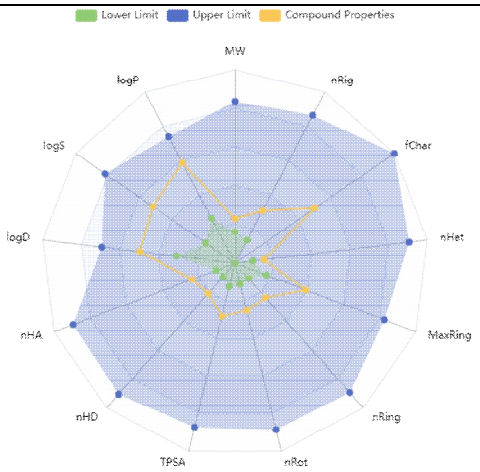

2-Methoxy-4-vinylphenol

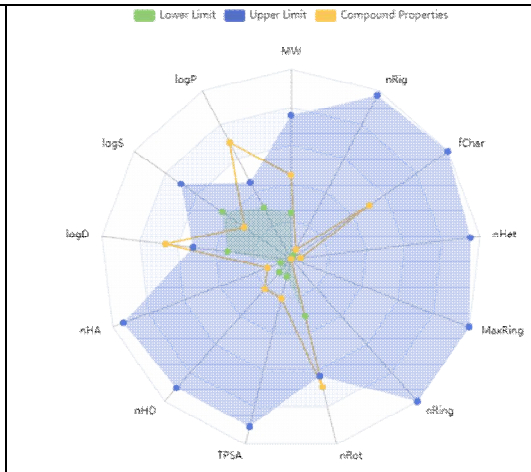

3,7,11,15-Tetramethyl-2-hexadecen-1-ol

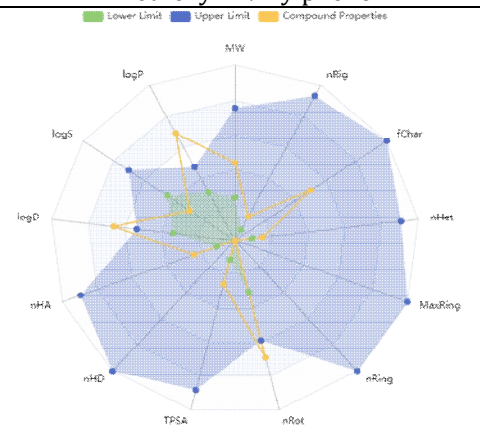

9,12-Octadecadienoic acid, methyl ester

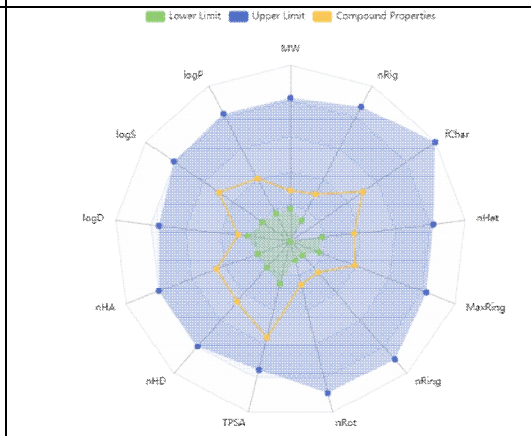

Benzoic acid, 3,4,5-trihydroxy-, methyl ester

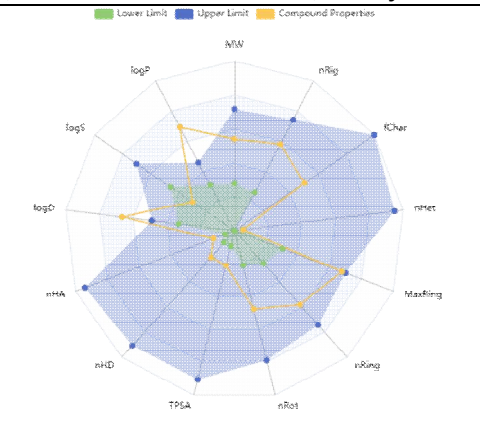

Campesterol

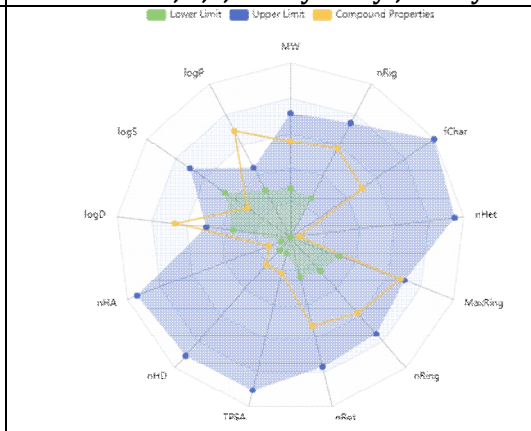

Gamma Sitosterol

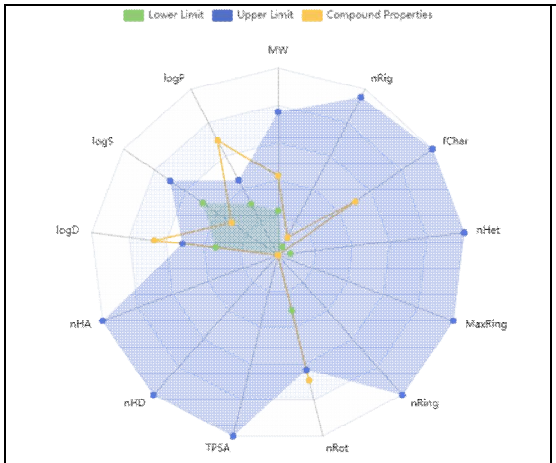

Neophytadiene

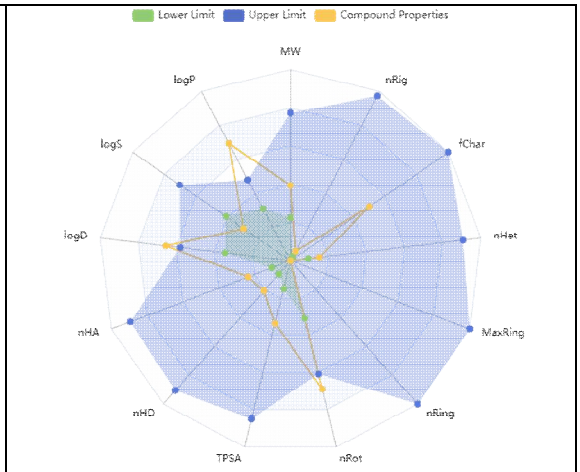

n-Hexadecanoic acid

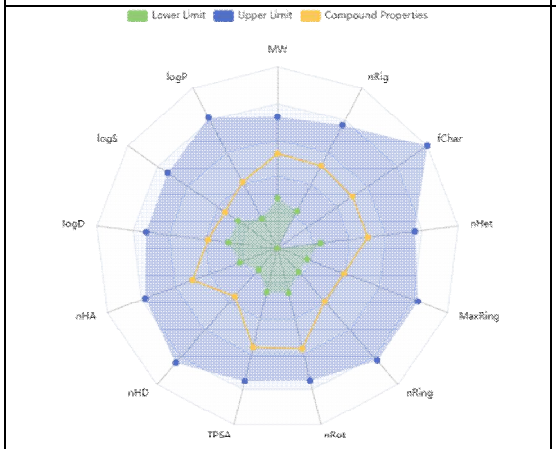

Pentanoic acid, 3-methyl-4-oxo

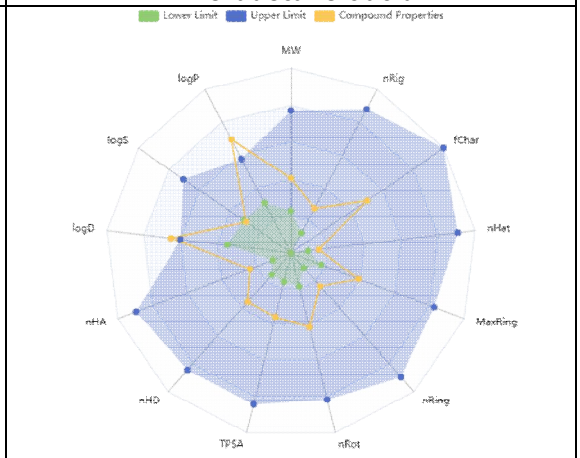

Phenol, 3,5-bis(1,1-dimethylethyl)

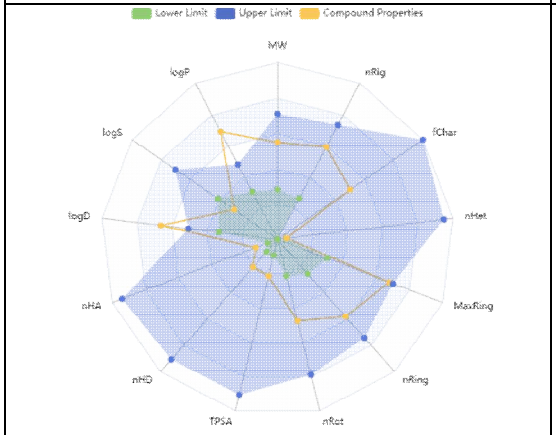

Stigmasterol

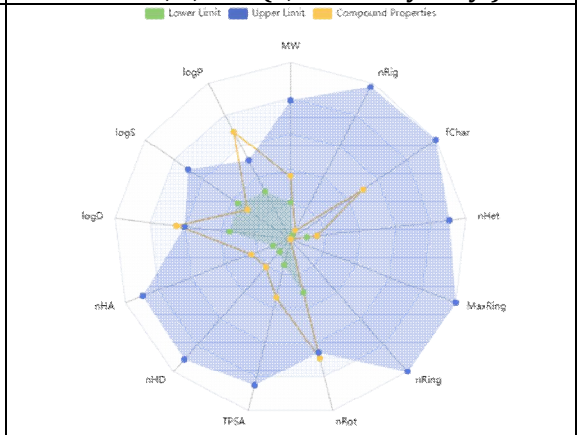

Tetradecanoic acid

CONCLUSION

The present study evaluated the phytochemical composition, physicochemical properties, microbial safety, and in silico therapeutic potential of *Cissus verticillata* extract. The hydroalcoholic extraction yielded a considerable number of bioactive constituents, and physicochemical parameters confirmed the identity, purity, and stability of the extract. The absence of heavy metals, pesticide residues, and pathogenic microorganisms indicates its safety for pharmaceutical applications. qualitative

phytochemical screening revealed the presence of multiple secondary metabolites, with phenolics and flavonoids as major constituents, suggesting strong antioxidant potential. GC–MS analysis further confirmed the presence of phenolics, fatty acids, terpenoids, and phytosterols, indicating rich chemical diversity. Molecular docking studies demonstrated that phytosterols such as stigmasterol, campesterol, and γ-sitosterol exhibited strong binding affinity toward DPP-IV, suggesting potential antidiabetic activity. ADMET analysis indicated that phenolic compounds possess better pharmacokinetic profiles, while sterols showed high binding affinity but limited solubility. Overall, *Cissus verticillata* is a promising source of bioactive compounds with potential therapeutic application. Further experimental validation and isolation of active compounds are recommended for drug development.

REFERENCES

1. Accili D, Deng Z, Liu Q. (2025). Insulin resistance in type 2 diabetes mellitus. Nat. Rev. Endocrinol., 21, 413–26 https://doi.org/10.1038/s41574-025-01114-y.
2. Alam S, Aijaz M. (2024). Complications of Cardiovascular Disease: The Impact of Diabetes, Dyslipidemia, and Metabolic Disorders. World J. Pharm. Res. 321. SJIF Impact Factor 8, 13.
3. Satyam Mishra, Pooja Tiwari, Rubi Yadav, Pratixa S Patel. An Extensive Analysis of Diseases Associated with Diabetes. J. Pharma Insights Res., 2, 174–87 (2024) https://doi.org/10.69613/ng1j7s13.
4. Suryavanshi S V., Kulkarni YA. NF-κβ: A potential target in the management of vascular complications of diabetes, 2017.
5. Król M, Kupnicka P, Żychowska J, Kapczuk P, Szućko-Kociuba I, Prajwos E, Chlubek D. (2025). Molecular Insights into the Potential Cardiometabolic Effects of GLP-1 Receptor Analogs and DPP-4 Inhibitors. Int. J. Mol. Sci., 26, https://doi.org/10.3390/ijms26146777.
6. Kuthati Y, Davuluri VNG, Wong CS. (2025). Therapeutic Effects of GLP-1 Receptor Agonists and DPP-4 Inhibitors in Neuropathic Pain: Mechanisms and Clinical Implications. Biomolecules, 15, https://doi.org /10.3390 /biom15050622.
7. Abbas G, Akhtar MS, Haq QM, Al Amri IS, Wang D, Hussain H. (2025). Dipeptidyl peptidase IV inhibitors as a potential target for diabetes: patent review 2019–present,.
8. Olivares M, Hernández-Calderón P, Cárdenas-Brito S, Liébana-García R, Sanz Y, Benítez-Páez A. (2024). Gut microbiota DPP4-like enzymes are increased in type-2 diabetes and contribute to incretin inactivation. Genome Biol., 25, https://doi.org/10.1186/s13059-024-03325-4.
9. Suryaningtyas IT, Jung WK, Lee SJ, Je JY. (2025) Bioactive peptides PIISVYWK and FSVVPSPK improve glucose homeostasis by targeting DPP-IV and glucose transport in type 2 diabetic mice. Int. Immunopharmacol., 158, https://doi.org/10.1016/j.intimp.2025.114844.
10. Zhao R, Zhou Y, Shen H, Guan L, Wang Y, Shen X, Wang F, Yao X. (2025). Preparation and Encapsulation of DPP-IV Inhibitory Peptides: Challenges and Strategies for Functional Food Development, Foods. https://doi.org /10.3390/foods14091479
11. García-Curiel L, Berenice ORL, Elizabeth CGA, Emmanuel PE, Pérez-Flores JG, Guillermo GOL. (2025). DPP-IV Inhibitory Peptides From Whey Proteins: Production, Functional Mechanisms, Bibliometric Insights, and Future Directions for Type 2 Diabetes Therapy. Pept. Sci., 117, https://doi.org/10.1002/pep2.70000.
12. Chaachouay N, Zidane L. (2024). Plant-Derived Natural Products: A Source for Drug Discovery and Development. Drugs Drug Candidates, 3, 184–207 https://doi.org/10.3390/ddc3010011.
13. Delanogare E, Heberle RB, De Medeiros Barros W, Kraus SI, Braga SP, Machado AE, Dos Santos Barbosa LA, Dos Santos GJ, Biavatti MW, Faqueti LG, Da Silva LAL, Sandjo LP, Moreira ELG. (2025). The aqueous extract of *Cissus verticillata* leaves prevents diabetic allodynia in type 1 and type 2 diabetic mouse models regardless of glycemic control. Brazilian J. Pharm. Sci., 61, https://doi.org/10.1590/s2175-97902025e24621.
14. Millán-Aguilar O, Ordóñez-Rosas ML, Castillo-Cruz I, Rodríguez-Arredondo L, Ruiz-Domínguez M, Hurtado-Oliva MÁ, Manzano-Sarabia M. (2025). Nuisance Growth of *Cissus verticillata* (Vitaceae) Negatively Affects the Structure of Mangroves in Marismas Nacionales Nayarit, Mexico. Diversity, 17. https://doi.org /10.3390 /d17060407.
15. Taher MA, Kundu R, Laboni AA, Shompa SA, Moniruzzaman M, Hasan MM, Hasnat H, Hasan MM, Khan M. (2024). Unlocking the medicinal arsenal of Cissus assamica: GC-MS/MS, FTIR, and molecular docking insights. Heal. Sci. Reports, 7, https://doi.org/10.1002/hsr2.70091.
16. Mondal I, Zilani MNH, Lisany NF, Yasmin F, Bibi S, Biswas P, Tauhida SJ, Rahman MS, Albadrani GM, Al-Ghadi MQ, Sayed AA, Hasan MN, Abdel-Daim MM. (2025). C*issus quadrangularis* Revealed as a Potential Source of Anti-Inflammatory and Anti-Diabetic Pharmacophore in Experimental and Computational Studies. Chem. Biodivers., 22, https://doi.org/10.1002/cbdv.202500903.
17. Vijh D, Gupta P. (2024) GC–MS analysis, molecular docking, and pharmacokinetic studies on *Dalbergia sissoo* barks extracts for compounds with anti-diabetic potential. Sci. Rep., 14, https://doi.org/10.1038/s41598-024-75570-3.
18. Siddiqui Q, Shaikh YA. (2026). Hydroalcoholic Extraction of *Cissus quadrangularis* and In Vitro Evaluation of Antifungal Properties. J. PharmTechNova, 01, 3–10 https://doi.org/10.66220/vyc7rc95.
19. Siddiqui FA, Bakshi V. (2026). GC–MS-based analytical profiling of Lantana camara phytoconstituents and computational analysis for multi-target antidiabetic activity. J. Chem. Lett., 7, 1–24 https://doi.org/ 10.22034/

jchemlett.2026.571698.1375.
20. Sarma M Das. (2024). Different qualitative and quantitative analytical techniques for determination of major anthraquinonoids in Rhubarb. Chem. Rev. Lett., 7, 560–72. https://doi.org/10.22034/crl.2024.459167.1339.
21. Balta Y, Yerlikaya O. (2025). Determination of some physicochemical, microbiological, sensorial properties and vitamin B12 contents in kefirs by using biopreservative cultures. Food Biosci., 68. https://doi.org/10.1016/j.fbio.2025.106542.
22. Zhou J, Bilyera N, Guillaume T, Yang H, Li FM, Shi L. (2024). Microbial necromass and glycoproteins for determining soil carbon formation under arbuscular mycorrhiza symbiosis. Sci. Total Environ., 955. https://doi.org/10.1016/j.scitotenv.2024.176732.
23. Roy D, Roy D. (2026). Drug repurposing of some US FDA-approved drugs using Binding strength Studies for the Treatment of Methicillin- resistant *Staphylococcus aureus* Infection. J. Phytopharm. Adv. Chem., 01, 30–44. https://doi.org/10.66220/ecsrwe33.
24. Pardaev J, Sadikova U. (2026). Computational Study of Alkaloids Transferase as Antidiabetic Agents Targeting. J. Phytopharm. Adv. Chem., 01, 18–29. https://doi.org/10.66220/qpba0t94.
25. Siddiqui FS. (2026). Computational Assessment of Secondary Metabolites as Potential Inhibitors of Methylenetetrahydrofolate Dehydrogenase-2 (MTHFD2). J. Phytopharm. Adv. Chem., 2, 3–17. https://doi.org/10.66220/wwze8340.
26. Suryawanshi RM, Shimpi RB, Muralidharan V, Nemade LS, Gurugubelli S, Baig S, Vikhe SR, Dhawale SA, Mortuza MR, Sweilam SH, Siddiqui FA, Khan SL, Tutone M, Ahmad I, Begh MZA. (2025). ADME, Toxicity, Molecular Docking, Molecular Dynamics, Glucokinase activation, DPP-IV, α-amylase, and α-glucosidase Inhibition Assays of Mangiferin and Friedelin for Antidiabetic Potential. Chem. Biodivers., 22. https://doi.org/10.1002/cbdv.202402738.
27. Khan SL, Siddiqui FA, (2021). Jain SP, Sonwane GM. Discovery of Potential Inhibitors of SARS-CoV-2 (COVID-19) Main Protease (Mpro) from *Nigella Sativa* (Black Seed) by Molecular Docking Study. Coronaviruses, 2, 384–402. https://doi.org/10.2174/2666796701999200921094103.